



New **E**nabling **V**isions and Tools for **E**nd-use**R**s and stakeholders thanks to a common **M**Odeling app**R**oach towards a Climat**E** neutral and resilient society

D3.3 Analysis of impact models and planetary boundaries for the IAM

November 2023



This project has received funding from the European Union's Horizon Europe research and innovation programme under grant agreement No 101056858.

Document history

Project Acronym	NEVERMORE
Project ID	101056858
Project title	New Enabling Visions and Tools for End-useRs and stakeholders thanks to a common MOdeling appRoach towards a ClimatE neutral and resilient society
Project coordination	Fondazione Bruno Kessler (Italy)
Project duration	1 st June 2022 – 31 st May 2026
Deliverable Title	D3.4 Analysis of impact models and planetary boundaries for the IAM
Type of Deliverable	R – Document, Report.
Dissemination level	PU – Public
Status	Final
Version	1.0
Work package	WP3 – Climate science information
Lead beneficiary	PIK
Author(s)	Laura Bartolomé Quevedo (UVa), Noelia Ferreras Alonso (CARTIF), Stelios Karozis (NCSR), Paola Lopez Muñoz (UVa), Adrián Mateo Martínez (CARTIF), Iván Ramos (CARTIF), Jan Volkholz (PIK)
Reviewer(s)	Sofie Hellsten (IVL), Stelios Karozis (NCSR), Iván Ramos (CARTIF), Thanasis Sfetsos (NCSR), Alessia Torre (FBK)
Due date of delivery	30/11/2023
Actual submission date	30/11/2023

Date	Version	Contributors	Comments
22/05/2023	0.1	Noelia Ferreras Alonso (CARTIF), Paola Lopez Muñoz (UVa), Adrián Mateo Martínez (CARTIF), Iván Ramos (CARTIF), Jan Volkholz (PIK)	Table of Content (ToC) shared with reviewers and contributors
14/11/2023	0.2	Laura Bartolomé Quevedo (UVa), Noelia Ferreras Alonso (CARTIF), Stelios Karozis (NCSR), Paola Lopez Muñoz (UVa), Adrián Mateo Martínez (CARTIF), Jan Volkholz (PIK)	β-version ready for reviewers
24/11/2023	0.3	Laura Bartolomé Quevedo (UVa), Noelia Ferreras Alonso (CARTIF), Sofie Hellsten (IVL), Stelios Karozis (NCSR), Paola Lopez Muñoz (UVa), Adrián Mateo Martínez (CARTIF), Thanasis Sfetsos (NCSR), Jan Volkholz (PIK)	Final complete draft shared for review
27/11/2023	0.4	Laura Bartolomé Quevedo (UVa), Noelia Ferreras Alonso (CARTIF), Stelios Karozis (NCSR), Paola Lopez Muñoz (UVa), Adrián Mateo Martínez (CARTIF), Iván Ramos (CARTIF), Alessia Torre (FBK), Jan Volkholz (PIK)	Comments and feedback integrated
30/11/2023	1.0	Alessia Torre (FBK), Ivan Ramos Diez (CARTIF)	Final editing and submission



New Enabling Visions and Tools for End-useRs and stakeholders thanks to a common
MOdeling appRoach towards a ClimatE neutral and resilient society

Copyright ©2022 NEVERMORE Consortium Partners. All rights reserved.

NEVERMORE is a Horizon Europe Project supported by the European Commission under contract No.101056858. For more information on the project, its partners, and contributors please see NEVERMORE website. You are permitted to copy and distribute verbatim copies of this document, containing this copyright notice, but modifying this document is not allowed. All contents are reserved by default and may not be disclosed to third parties without the written consent of the NEVERMORE partners, except as mandated by the European Commission contract, for reviewing and dissemination purposes. All trademarks and other rights on third party products mentioned in this document are acknowledged and owned by the respective holders. The information contained in this document represents the views of NEVERMORE members as of the date they are published. The NEVERMORE consortium does not guarantee that any information contained herein is error-free, or up to date, nor makes warranties, express, implied, or statutory, by publishing this document.

Abbreviations and acronyms

Acronym	Description
AOD	Aerosol Optical Depth
BC	Black carbon
BII	Biodiversity Intactness Index
CAEs	Convolutional Autoencoders
CAP	Common Agricultural Policy
CMIP	Coupled Model Intercomparison Project
CNN	Convolutional Neural Networks
E/MSY	Extinctions per million species-year
EASOC	Southeast Asia & Oceania
EESC	Equivalent Effective Stratospheric Chlorine
EF	Emission factor
EPA	United States Environmental Protection Agency
ER	Emission efficiency of a given technology or sector
GA	Grant agreement
GCM	Global Climate Model
HANPP	Human Appropriation of the biosphere's NPP
IAM	Integrated Assessment Model
ISIMIP	Inter-Sectoral Impact Model Intercomparison Project
N	Nitrogen
NPP	Net Primary Production
OC	Organic carbon
ODS	Ozone depleting substance
OM	Organic matter
P	Phosphorous
pft	Plant functional type
ppm	Parts Per Million
SDM	System Dynamics Model
SSE	Sum of Squared Errors
SSP	Shared Socioeconomic Pathway
VEI	Volcanic Explosivity Index
VEII	Volcanic Explosivity Index Indicator
VMF	Variable Monthly Flow
WILIAM	Within Limits Integrated Assessment Model
WP	Work Package

Table of Contents

DOCUMENT HISTORY	1
ABBREVIATIONS AND ACRONYMS	3
TABLE OF CONTENTS	4
LIST OF FIGURES	5
LIST OF TABLES	5
EXECUTIVE SUMMARY	6
1. INTRODUCTION	6
2. CLIMATE ATTRIBUTION VARIABLES AND NATURAL PHENOMENA	7
2.1. Feature selection	8
2.2. Causality analysis	8
2.3. Climate attribution results.....	9
2.3.1. Volcanoes	9
2.3.2. Fires	12
3. ANALYSIS AND METHODS FOR THE USABILITY OF ISIMIP DATA	13
3.1. Assessment of climate change impacts using WILIAM	13
3.2. Introduction to ISIMIP	15
3.3. Description of the analysis of ISIMIP data for WILIAM	15
3.4. Description of variables	18
3.4.1. Climate variables	19
3.4.2. Crop yields	22
3.4.3. Biodiversity	23
3.4.4. Burnt areas	24
3.4.5. Evapotranspiration	24
3.4.6. Methane emissions	25
3.4.7. Forestry NPP	25
3.5. Downscaling method for ISIMIP data	26
4. PLANETARY BOUNDARIES	26
4.1. Introduction into planetary boundaries	27
4.2. Description of the planetary boundaries	29
4.3. Current status at WILIAM and modelling proposals for each planetary boundary ..	33
4.4. Conclusions on planetary boundary modelling in WILIAM	37
5. CONCLUSIONS	39
6. REFERENCES	40

List of Figures

Figure 1. Workflow of climate attribution analysis.	7
Figure 2. Prediction of CO2 contribution based on fitted parameters of volcanoes.	11
Figure 3. Prediction of CO2 contribution based on fitted parameters of fire parameters.	13
Figure 4. WILLIAM regions. Source: (Pastor, et al., 2021).	19
Figure 5. Low extreme values (5th percentiles) of tas.	20
Figure 6. Median values (50th percentiles) of tas.	21
Figure 7. High extreme values (95th percentiles) of tas.	21
Figure 8. Median values (50th percentiles) of tasmin.	21
Figure 9. Median values (50th percentiles) of tasmax.	22
Figure 10. Median values (50th percentiles) of pr.	22
Figure 11. Planetary Boundary Framework, showing two of the many potential types of relationships between a control and response variable. Source: (Gleeson, et al., 2020).	27
Figure 12. Average forestry boundaries of nations during 1991–2015. Source: (Zhang et al., 2021) ..	31
Figure 13. The core functions of water in the Earth System (larger diagram) and how they are represented in the current freshwater use planetary boundary (small diagram). Source: (Gleeson, et al., 2020).	32
Figure 14. Emissions, Total Mass Burden and AOD by Region for 2001. Source: (Streets, et al., 2009).	34
Figure 15. Model estimated relationship between emission (E) and surface concentrations (C) (black dots) or AOD (A) (blue crosses) of SO ₂ , OM and BC on regional and annual average over different regions. Source: (Chin, et al., 2014)	35
Figure 16. Schematic of the definition of HANPP used in Richardson et al. (2023), (not to scale) Source: (Richardson, et al., 2023), supplementary material.	37

List of Tables

Table 1. Top 40 Mallow’s Cp scores for volcanoes contribution to climate change. Source: Own elaboration.	10
Table 2. Causality analysis of Volcanoes related variables. Source: Own elaboration.	11
Table 3. Mallow’s Cp scores for fire contribution to climate change. Source: Own elaboration.	12
Table 4. Causality analysis of fire related variables. Source: Own elaboration.	12
Table 5. Summary of NEVERMORE ISIMIP dataset.	19
Table 6. ISIMIP climate data.	20
Table 7. ISIMIP crop yield data.	23
Table 8. ISIMIP biodiversity data.	23
Table 9. ISIMIP burnt area data.	24
Table 10. ISIMIP evapotranspiration data.	24
Table 11. ISIMIP methane emission data.	25
Table 12. ISIMIP forestry NPP data.	25
Table 13. Summary of all planetary boundaries and proposed control variables. The control variables marked with an asterisk * are those proposed as an alternative or complement to the control variables proposed in Rockström et al. (2009) and Steffen et al. (2015).	37

Executive summary

Task 3.3 “Analysis of climate change impact models and assessment of planetary boundaries and other control variables” deals mainly with the improvement of the integrated assessment model (IAM) WILIAM. IAMs are tools that offer a holistic picture of the complex relationships among different human and environmental sectors. They integrate the interactions between economy, energy, water, climate change or land use, among other sectors, assessing future projections and aiming at supporting policymakers to develop sound policies. Besides this aspect there is also a smaller side task exploring the translation of coarse data to more detailed scales (case studies). To improve WILIAM in the future, also in other WP of the project, a methodology based on causality analysis for the climate attribution and level of impact of natural, extreme or other rare events is described. Here the method is applied to volcanoes and fires, and it was found fit for its intended purposes.

Another way to refine WILIAM is the analysis and the development of a method for the incorporation of ISIMIP data into WILIAM. ISIMIP¹, the Inter-Sectoral Impact Model Intercomparison Project, collects data from models that simulate the impacts of climate change on various sectors such as rivers, forests or agriculture. To condense this knowledge for WILIAM we give the median as well as the extremes of a variety of variable ensembles, 19 of them, at different levels of global warming. Examples of the variables we analysed are temperatures, crop yields, number of bird species, and methane emissions. Related is one task that does not focus on enhancing WILIAM: the exploration of the downscaling of ISIMIP data via deep learning. This is based on convolution autoencoders with evidence transfer architecture that allows external properties to be considered (e.g. land properties) in the parameters downscaling. The approach has been used in Task 3.2 “Downscaling of climate information” for climate datasets and it will be tested in some ISIMIP variables.

Furthermore, we investigate how the handling of planetary boundaries can be improved in WILIAM. For each of these boundaries a literature study was carried out, and suitable variables and possible modelling enhancements were pondered and weighted. While it turned out that one of them (novel entities) is borderline impossible to implement we found suitable control variables and their respective threshold values for all the remaining ones.

The work on this task/deliverable was jointly carried out by “Fundación CARTIF” (CARTIF), the “National Centre For Scientific Research Demokritos” (NCSR), the “Potsdam Institute for Climate Impact Research” (PIK), “RINA-Consulting” (RINA-C) and the “University of Valladolid” (UVa). “Fondazione Bruno Kessler” (FBK), CARTIF, NCSR, and the “Swedish Environmental Research Institute” (IVL) supported us by reviewing this document.

1. Introduction

Task 3.3 is embedded in WP3 “Climate science information” of the NEVERMORE project. This WP has two major foci. One of them is the exploitation of existing climate information to deliver climate high resolution datasets to feed the assessment of impacts and risks at case study level while the second one is the improvement of the integrated assessment model (IAM) WILIAM. It is the latter that we mostly deal with in Task 3.3. As a reminder, IAMs are models that capture the most important aspects of society, economy and the environment in broad strokes to support decision makers in developing sound and useful policies.

The aim of Task 3.3 is the analysis of climate change impact models and the assessment of planetary boundaries and other control variables. This task is to analyse and provide a method to use information from global sectoral impact models and to include the planetary boundaries framework as control

¹ www.isimip.org

variables into the modelling for supporting policy (in synergy with Task 3.4 “Uncertainty assessment and tipping points of climate scenarios”). Three main activities are carried out:

1. Perform a climate attribution of variables and level of impact are assessed by performing causality analysis, such as causality neural networks or detrended climate data. The case of natural phenomena (e.g. fires, volcanoes) is studied in relation to CO₂ emissions and land use changes.
2. Carry out an analysis and develop a method for the usability of ISIMIP global data for modelling, emulating, calibrating and validating climate change impacts on biogeochemical and hydrological processes in WILIAM (Task 4.2 “Methodology for climate change assessment including impacts and risks”, Task 4.3 “Design and modelling of impacts and risks on the different dimensions”) while assuring scenario consistency (Task 4.1 “Scenarios coherence across scales”). To recap once more, the ISIMIP Project collects data from models that simulate the impacts of climate change on various sectors such as agriculture, global fisheries or health. For a more thorough description of ISIMIP see Section 3.2. The generated data also provide a baseline of extreme event for the IAM and regions under study. A downscaling of ISIMIP data (mostly on a 0.5°×0.5° grid) for the case studies analysis via deep learning techniques is explored as well.
3. Investigate and develop methods for including planetary boundaries in WILIAM via the assessment and the definition of “safe” values of specific variables.

The above description is essentially the task description from the GA.

In order to work on these topics, the task leader PIK in close collaboration with the partners from CARTIF, NCSR, RINA-C and UVA regularly held video conferences throughout the task’s duration and did a physical workshop in May 2023 in Valladolid to ensure smooth progress in reaching this task’s objectives.

The first subtask of Task 3.3, the climate attribution, is dealt with in Section 2. It describes in detail how the climate attribution was carried out and how it was applied to fires and volcanoes.

The second subtask entails two different objectives. In the first ISIMIP data are analysed and then condensed into a usable format for WILIAM. In Sections 3.3 and 3.4 we describe the algorithm used and explain for every variable what has been done exactly. In the second we explored the downscaling of ISIMIP data via deep learning. The efforts spent on this are reported in Section 3.5.

The final Section 4 deals with the work done on the planetary boundaries. That section introduces planetary boundaries and describes in detail various options of how their handling in WILIAM can be implemented respectively be improved.

2. Climate attribution variables and natural phenomena

Under the scope of the NEVEREMORE project and the enhancing of the capabilities of the IAM model WILIAM, a method was developed under Task 3.3 to provide information about the climate attribution of extreme events or rare phenomena, such as volcanoes and fires. The approach is based on a causality analysis of different variables to CO₂ global emissions. The workflow consists of (a) data fusion and engineering, (b) feature selections analysis (filter what variables should be used in the causality analysis), (c) causality analysis and (d) development of relevant function. Figure 1 shows the steps followed in the climate attribution.



Figure 1. Workflow of climate attribution analysis.

2.1. Feature selection

When there is a set of potential predictor variables, it is essential to select the most informative subset of features to build a useful model. To help choose the best subset of features in the context of climate attribution, the statistical criterion Mallows' C_p was used. It is based on the concept of model fit and the trade-off between model complexity and goodness of fit (Moore et al., 2014). The goal is to find a balance between a model that fits the data well and a model that is not too complex. The formula for Mallows' C_p is as follows (Equation 1):

$$C_p = (SSE_p/s^2) - (n - 2p)$$

Equation 1

Where:

C_p is Mallows' C_p statistic for a specific model with p predictor variables.

SSE_p is the sum of squared errors for the model with p predictor variables.

s^2 is the estimated variance of the error term in the full model with all available predictors.

n is the number of data points (sample size).

The idea behind the method is to compare the quality of the fit with p predictors against the fit with all available features. It quantifies the difference between the two, taking the number of predictors in the reduced model into account. A model with a lower C_p value is preferred because it indicates a good balance between model fit and simplicity. However, it is important to note that the final choice of predictors should also consider other factors, such as theoretical knowledge and the context of the problem (Moore et al., 2014; Burnham & Anderson, 2002; Agresti & Finlay, 2009; James et al., 2013).

2.2. Causality analysis

Causality analysis in datasets aims to understand and establish causal relationships between variables or factors. It involves determining whether changes in one variable cause changes in another. Causality analysis is a fundamental aspect of statistical and scientific research, and it is often conducted using various methods and approaches. It is essential to distinguish between correlation and causation. Correlation indicates a statistical relationship between two variables, while causation suggests that changes in one variable led to changes in another. Correlation does not imply causation.

In the current study the Granger causality test is used. It is a statistical hypothesis test used to determine whether one time series can predict another. The Granger causality principle is based on the idea that if one time series X "Granger-causes" another time series Y , then past values of X should contain information that helps predict Y better than when past values of Y alone are used.

One parameter that current test is using involves the selection of past observations of X and Y should be included in the analysis. The latter it is called the order of Time Lags and for the current study 1 and 2 were tested in each case.

In addition, since phenomena like volcanoes and fires cannot be described with one variable or indicator, the Granger causality test is used in conjunction with Vector Autoregressive (VAR) models, which model multivariate time series data to study causal relationships between variables (Granger & Newbold, 1974; Granger, 1969; Engle & Granger, 1974; Hamilton, 1994).

2.3. Climate attribution results

In this task the climate attribution and level of impact of volcanoes and fires has been explored. In particular, the “volcanoes” have been used as a toy model where the method has been validated. However, final applicability of the functions to be obtained ought to be preliminarily studied in order to prioritize what we need to include in WILIAM in this project. In particular, NEVERMORE is focused on climate change impacts and risks, as well as on effects that could be mitigated via adaptation functions (adaptation policies). According to this aspect, functions obtained in relation to fires have been selected to be potentially integrated in WILIAM in relation to risk assessment. Other candidates are the modelling of climate change impacts in WILIAM and adaptation measures that could mitigate them (e.g. forest management) (links with Task 4.2 “Methodology for climate change assessment including impacts and risks”).

In this regard, the result of causality analysis will yield a function that can be used in more than one way in the NEVERMORE project:

1. IAM integration: Utilize the provided function in WILIAM model and fully integrate them into the climate module.
2. Scenario building: Use the function to develop scenarios and input variable for WILIAM.
3. ICT Toolkit: Utilise the function in Gamification as randomly occurring extreme events to explore the effect in the finale time series scenario.

2.3.1. Volcanoes

For the case of climate attribution of volcanoes eruptions to the climate condition, a dataset was built from two sources of observations: (a) from the volcanoes activity database of National Museum of Natural History – Smithsonian Institution, and (b) from Manua Loa Observatory of NOAA Global Monitoring Laboratory CO₂ measurements. The datasets were fused for the common years, resulting in a time series covering the period of 1960–2022 (Tans, 2023; Keeling, 2023). The available variables include:

- Er. Total: Number eruption of the year.
- Volcanoes Active: Number of active volcanoes.
- Er. Started: Number of new eruptions.
- Er. Ended: Number of eruptions ended.
- VEI ≤ 2: Volcanic Explosivity Index (VEI) less than or equal to 2.
- VEI 3: Volcanic Explosivity Index (VEI) equal to 3.
- VEI 4: Volcanic Explosivity Index (VEI) equal to 4.
- VEI 5: Volcanic Explosivity Index (VEI) equal to 5.
- VEI 6: Volcanic Explosivity Index (VEI) equal to 6.

In case of (a) the number of eruptions per year and the Volcanic Explosivity Index (VEI) was included. During the analysis a feature engineering action was performed by creating an average VEI indicator (VEII) with a weighted average formula (Equation 2).

$$VEII = VEI_{\leq 2} + 10 \cdot VEI_3 + 100 \cdot VEI_4 + 1000 \cdot VEI_5 + 10000 \cdot VEI_6$$

Equation 2

As described in the beginning of the section, a feature selection was applied with all the combination of variables available, see Table 1. The results yield the most prominent variables that will be used for the causality analysis. The prominent variables and the causality analysis can be found in Table 2.

Table 1. Top 40 Mallow's Cp scores for volcanoes contribution to climate change. Source: Own elaboration.

VEI12	Er. Total	Volcanoes Active	Er. Started	Er. Ended	VEI <=2	VEI 3	VEI 4	VEI 5	VEI 6	CP
		✓	✓							0.520
	✓	✓	✓							0.843
	✓	✓	✓	✓						1.684
		✓	✓					✓		1.955
		✓	✓				✓			2.325
		✓	✓	✓						2.382
✓		✓	✓							2.387
	✓	✓	✓					✓		2.393
		✓	✓						✓	2.453
		✓	✓		✓					2.458
		✓	✓			✓				2.475
	✓		✓	✓						2.583
	✓	✓	✓				✓			2.763
	✓	✓	✓		✓					2.786
	✓	✓	✓			✓				2.787
	✓	✓	✓						✓	2.837
✓	✓	✓	✓							2.840
	✓	✓	✓							3.191
✓	✓	✓	✓					✓		3.249
		✓			✓	✓				3.413
	✓	✓	✓	✓		✓				3.575
	✓	✓	✓	✓	✓					3.600
	✓	✓	✓	✓			✓			3.643
	✓	✓	✓	✓					✓	3.677
✓	✓	✓	✓	✓						3.682
	✓	✓					✓	✓		3.801
	✓	✓	✓					✓		3.806
	✓	✓		✓				✓		3.880
	✓	✓				✓		✓		3.939
✓		✓	✓					✓		3.951
		✓	✓					✓	✓	3.954
	✓	✓			✓	✓				4.126
✓		✓	✓						✓	4.148
		✓			✓	✓		✓		4.170
		✓	✓	✓			✓			4.191
✓		✓	✓				✓			4.213
✓		✓	✓	✓						4.218
✓	✓	✓	✓					✓		4.244

✓	✓	✓				✓	✓	4.260
	✓	✓			✓		✓	4.283

Table 2. Causality analysis of Volcanoes related variables. Source: Own elaboration.

Model	lag	p-value	Causality (p-value < 0.05)
VEI12 - CO2	1	0.910	✗
	2	0.119	✗
Eruptions Total - CO2	1	7.638e-05	✓
	2	0.005	✓
Volcanoes_Active - CO2	1	2.788e-05	✓
	2	0.0007	✓
Eruptions Started - CO2	1	0.100	✗
	2	0.2906	✗
Eruptions Ended - CO2	1	0.0005	✓
	2	0.0184	✓

The causality analysis provided the evidence on which variables play a role in CO₂ emission. The analysis also provides a relation function with Eruption_Total, Volcanoes_Active and CO₂ emissions that can be found below as the Equation 3. The Figure 2 shows the representation of the predicted and the actual CO₂ emissions due to volcano activity with the chosen parameters.

$$x_1 = \text{Eruptions Total}$$

$$x_2 = \text{Volcanoes Active}$$

$$y = -1.33(\pm 1.14)x_1 + 4.49(\pm 1.36)x_2 + 165.78(\pm 17.6)$$

Equation 3

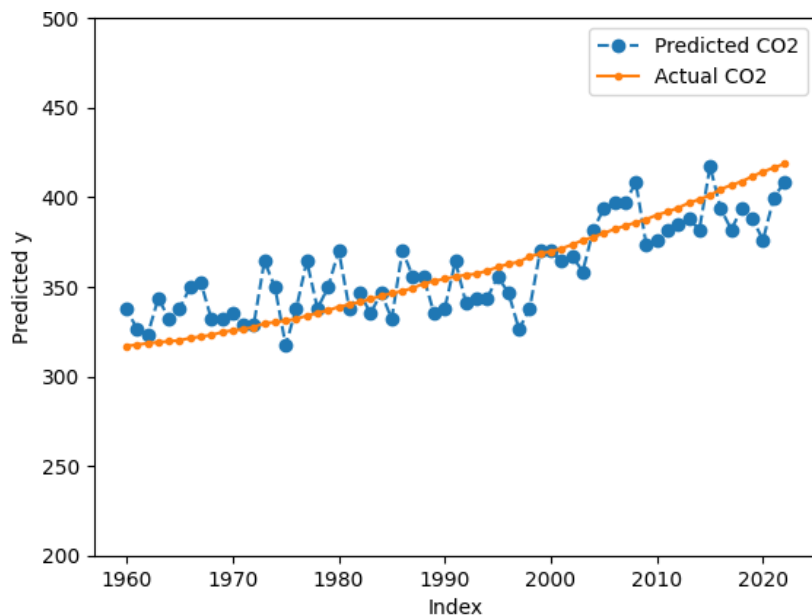


Figure 2. Prediction of CO₂ contribution based on fitted parameters of volcanoes.

2.3.2. Fires

For the case of fires, the ISIMIP database was used to extract fires related variables². The ISIMIP database offers gridded dataset that were statistical post-processed in the current section for producing spatial average and maximum values. The variables used were:

- *burntarea-total*: Global average of Burnt Area Fraction.
- *ffire-total*: Global average of carbon Mass Flux into Atmosphere due to C Emission from all fires.
- *landalbedo*: Global average of Surface Albedo of Land.
- *burntarea-total-max*: Global maximum of Burnt Area Fraction.
- *ffire-total-max*: Global maximum of Mass Flux into Atmosphere due to C Emission from Fire.
- *landalbedo-max*: Global maximum of Surface Albedo of Land.

For assessing what combination of variables to use in the causality analysis, the Mallow’s Cp score was used. The outcome yields three prominent variables to be checked in the causality analysis, *burntarea-total-max*, *ffire-total-max* and *landalbedo-max*. All the Mallow’s Cp scores can be found in Table 3.

Table 3. Mallow’s Cp scores for fire contribution to climate change. Source: Own elaboration.

Burnt-area-total	ffire-total	Land-albedo	Burnt-area-total-max	ffire-total-max	Land-albedo-max	CP
			✓			0.61
			✓	✓		1.17
			✓		✓	1.31
✓			✓			1.65
✓			✓	✓		1.99
			✓	✓	✓	2.15
✓			✓		✓	2.48
		✓	✓			2.50
	✓		✓			2.61
		✓	✓	✓		2.98
				✓		3.04
✓			✓	✓	✓	3.12
	✓		✓	✓		3.15

For the prominent variables the Granger causality test was applied. The test resulted to only one variable that has a causal relation to CO₂ emissions, the Burned Area max as can be seen in Table 4.

Table 4. Causality analysis of fire related variables. Source: Own elaboration.

Model	Lag	p-value	Causality (p-value < 0.05)
Burnt Area max - CO2	1	0.033	✓
	2	0.110	✗
Ffire max - CO2	1	0.116	✗
	2	0.178	✗
Landalbedo max - CO2	1	0.226	✗
	2	0.194	✗

²ISIMIP2b / Historical outputs / Model: UKESM1-0-LL / Monthly data

For Burnt Area Max the function that provide the relation with CO₂ emissions can be found below (Equation 4). The prediction of CO₂ contribution is shown in Figure 3.

$$x = \text{Burned Area max}$$

$$y = -6.12(\pm 3 \cdot 10^{-7})x + 361.96 (\pm 5.76)$$

Equation 4

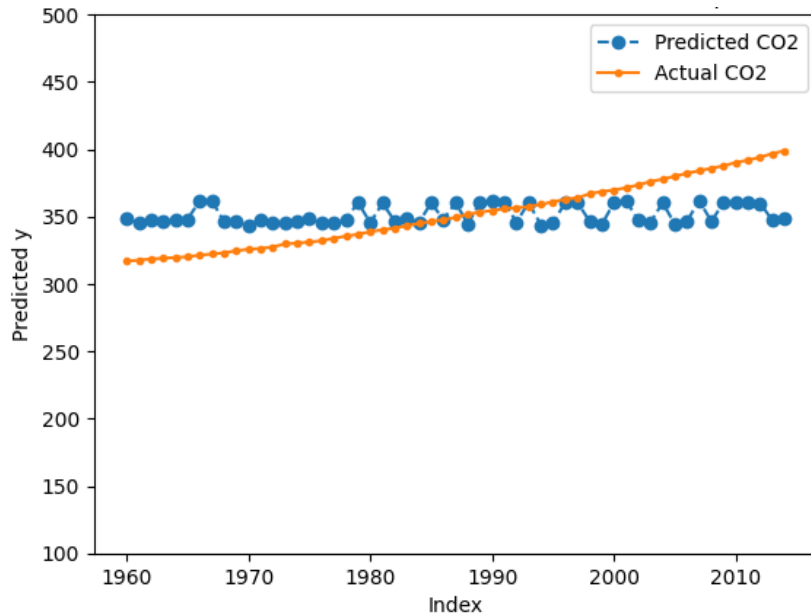


Figure 3. Prediction of CO₂ contribution based on fitted parameters of fire parameters.

3. Analysis and methods for the usability of ISIMIP data

The analysis of ISIMIP data, see Section 3.2, 3.2 and their harnessing for the improvement of WILIAM is a major point in Task 3.3. In this section we describe the method we devised in detail to achieve this goal and we describe the variables we have analysed.

3.1. Assessment of climate change impacts using WILIAM

Before delving into the analysis of ISIMIP data, it is necessary to understand the application and objective of this assessment. Therefore, a preliminary strategy on how we are going to use this information and where it is needed is described in this section. As commented above, the objective is to model biophysical impacts in WILIAM by using information from sectoral impact models. In this regard, ISIMIP contains precise, public and well-organized results from a multitude of impact models in various sectors which allows for the application of a general methodology for impacts to more than one sector.

WILIAM is a system dynamics model in which many of the relationships are endogenous and continuous, and that is why we need mathematical functions relating different variables. In this regard, when applied to the effects of climate change impacts, these relations are normally called “damage functions”, which normally in IAMs relates the global temperature (new climate condition) to a specific sectoral impact variable, such as crop yields.

The term “damage function” refers to a mathematical equation obtained from a regression analysis. This method is commonly used to include climate change impacts within computational models such as IAMs, which are usually models with a reduced level of detail. In this way, very specific computational models of different nature, which describe in great detail the physical impact to be

modelled (this way of modelling the impact is called process-based (Neumann et al., 2020)), are used to obtain data to estimate simple damage functions that are then incorporated into the IAM models.

The damage function, therefore, relates "the damage" (dependent variable) to one or more explanatory variables of the damage (independent variables), which are usually climatic variables.

This type of function is widely used in the economic field to link the increase in global or regional temperature (or changes in the patterns of climatic variables) with the impact on economic variables such as GDP or production factors (Piontek et al., 2019). However, it is still a generic method that can be used and is used in other fields of application (Koellner & Scholz, 2008).

When generating a damage function, it is necessary to proceed by the classical methods of calculating statistical regression models: a functional form must be proposed, whose parameters may have a theoretical meaning within the scope of application or not. It must be justified that there is indeed a relationship between the dependent variable and the independent variables, through some kind of statistical analysis of the data (such as a principal component analysis). And, as in any statistical study, the regression model must be validated, demonstrating that there is statistical significance of the parameters and that the model can predict within error tolerances.

A topic of great importance in this field is the analysis of the uncertainty of both the damage function and the model that employs it. It is necessary to define exactly the assumptions under which the regression model is valid, as well as to provide information on its statistical uncertainty. Models using these damage functions are usually subjected to some form of sensitivity analysis (Mechler et al., 2019).

These relations can be extracted from sectoral impact models focused on a sector, e.g. agriculture, which are able to model the climate change impacts on specific variables in great detail (e.g. different types of crops, data on a 0.5°×0.5° grid etc.) (Snyder et al., 2020).

Based in addition on the analysis of literature done in Deliverable 6.3 "Impact assessment considering social, environmental and economic aspects" from LOCOMOTION, most of them covering impacts on crops, where some specific climate change damage feedbacks were analysed and preliminarily defined according to the state-of-the-art, we here propose a methodology for exploiting the ISIMIP database which allows to collect public impact data from different sectoral models, applying the methodology to several biophysical sectors. In this regard, it is important to take the WILIAM sectors into account before designing a damage function (Pastor, et al., 2021).

The general method to be applied is the following:

- Extraction of the specific variable at different warming levels from the specific sectoral impact model.
- Aggregation to the spatial resolution of WILIAM (in this case: global regions and European countries).
- From the data processed from ISIMIP, extraction of the relations that allow to parametrize the factors to be applied to the variable modelled in WILIAM, to reflect the impacts of new climate conditions (climate scenarios). This generates the "damage function".

The damage functions obtained here allow to include many variable projections according to the evolution of the global temperature, which is the main endogenous indicator we are using as a reference. The way in which the functions were obtained guarantees that our mathematical relationships only cover isolated effects of climate change so that we do not incur in double-accounting, since socioeconomic and land-use effects in WILIAM are modelled via other methods and not by relying on ISIMIP data.

The way in which the algorithm produces the data is designed to ensure its consistency with WILIAM data needs. The methodology is aligned with Task 4.2 "Methodology for climate change assessment

including impacts and risks". The complete integration of the outputs obtained in this task will be done in the following months in the scope of Tasks 4.3 "Design and modelling of impacts and risks on the different dimensions" and 4.5 "Integration in the IAM considering future feedbacks and cascading effects and validation".

3.2. Introduction to ISIMIP

The *Inter-Sectoral Impact Model Intercomparison Project* (ISIMIP) is a project, run at the PIK that collects results from impact models in various sectors and makes the results available to the public. The central idea of ISIMIP is that all impact models are driven by the same data, i.e. the impact models use the same climate (temperatures, precipitation ...) and socioeconomic (population, land-use ...) data as their input. Sectors are various subsystems of the Earth and society, such as agriculture, fires, forests, marine fisheries, permafrost, hydrology and so on. By driving all impact models with the same curated data and scenarios the outcome of the model runs can be compared and put into perspective. A detailed specification of all variables and scenarios in the ISIMIP protocols guides the modellers and ensures consistency.

The ISIMIP project started in 2012 and is currently in its third round. Each of these rounds consists of two parts:

1. The first part focuses on model validation by providing observed climate and socioeconomic data as impact model drivers. This is labelled as "a", e.g. we speak of ISIMIP3a.
2. The second part collects climate and socioeconomic projections as driving data. With these drivers the impact models can project impacts in their respective sectors. In this case the label is "b" ("ISIMIP3b").

In order to get more robust statistics, we analyse impact data from two ISIMIP rounds, ISIMIP2 and ISIMIP3. The concepts of both rounds are very similar, but their driver data stem from different generations. For instance, while the climate data in the third round ISIMIP3b are based on CMIP6 data (Eyring, et al., 2016), the climate data in ISIMIP2b are based on CMIP5 runs (Taylor et al., 2012).

The second round of ISIMIP experiment setup, more specifically its "b" part, is described in Frieler et al. (2017). The protocol paper for ISIMIP3b is still being worked on, but an online version is available at the ISIMIP website³. For the ISIMIP3a protocol paper a preprint is already available at the Copernicus website⁴. All modelling results are available freely and can be downloaded by researchers, stakeholders and all other interested parties.

3.3. Description of the analysis of ISIMIP data for WILIAM

Analysing ISIMIP for WILIAM is not straightforward because both use completely different frameworks to describe a changing world. While the ISIMIP framework describes the climate and socioeconomics in terms of RCPs and SSPs, WILIAM uses scenarios apart from the Business as Usual, others such as a Green Growth (aligned with an SSP1), or Degrowth (more aligned with a high mitigation scenario). In order to make a connection between these two approaches we decided to use the global warming level, as compared to preindustrial times, as a link. PIK provides the data calculated with respect to the WILIAM region and the warming level. More precisely the median as well as low (5th percentile) and high extremes (95th percentile) are given. This way, the entire uncertainty span of the model ensemble is provided.

Another basic decision that was to be made was the selection of the ISIMIP experiment group. In ISIMIP there are several experiment setups prescribed. A basic distinction between these setups is how

³ <https://protocol.isimip.org/>

⁴ <https://egusphere.copernicus.org/preprints/2023/egusphere-2023-281/>

socioeconomic drivers are handled. One set of simulations varies both climate and socioeconomic drivers. This allows for model verification as well as projections of what might possibly happen in the future. Another modelling setup varies the climate only while leaving socioeconomic drivers constant. These runs allow to investigate the pure effect of a changing climate. In the discussions with the WILIAM team it turned out that the focus on the pure climate change effect is the most appropriate approach for WILIAM, and thus it was decided to base the analysis on ISIMIP runs with fixed socioeconomic conditions. Consequently, we chose ISIMIP2b runs with the 2005soc (all of socioeconomic is fixed at 2005 values) and the ISIMIP3b runs with 2015soc (all of the socioeconomic are fixed at 2015 values) scenarios. Regarding the CO₂ values, the scenarios with varying CO₂ were chosen.

At the workshop in Valladolid, where the teams of WILIAM and ISIMIP met, a set of ISIMIP variables that are interesting for WILIAM was identified.

In general, the algorithm follows along these lines:

1. As stated before, in ISIMIP the impact models are driven with climate data from various GCMs (ISIMIP2b: GFDL-ESM2M, HadGEM2-ES, IPSL-CM5A-LR, MIROC5; ISIMIP3b: GFDL-ESM4, IPSL-CM6A-LR, MPI-ESM1-2-HR, MRI-ESM2-0, UKESM1-0-LL). Besides simulating the historical climate as well as climate projections, each GCM also simulates an artificial surrogate climate where the atmosphere has the same composition as it had in preindustrial times. The climate models produce long running climate series (several hundred years) with this atmosphere. With this data it is possible to calculate the mean global preindustrial temperature for each GCM. As mentioned above, the GCMs also produce climate simulations for historic times and for climate projections. In ISIMIP we provide for each GCM historic climate runs (ISIMIP2b: 1861 to 2005; ISIMIP3b: 1850 to 2014) as well as climate projections (ISIMIP2b: RCP2.6, RCP6.0 and RCP8.5 from 2006 to 2099 resp. 2299; ISIMIP3b: SSP126, SSP370 and SSP585 from 2016 to 2100). For each year in these climate simulations, we can calculate the global mean temperature and compare it to the mean temperature of the GCM's preindustrial run. This way we can assign to each simulated year a warming level compared to preindustrial times.
2. We have decided to consider warming levels 0.0 °C, 0.25 °C, 0.5 °C, ..., 4.0 °C, 4.25 °C. Now we put each year into their respective warming level bins, e.g. all simulated years with a global warming $0.625\text{ °C} \leq \Delta T < 0.875\text{ °C}$ are put into the $\Delta T = 0.75\text{ °C}$ bin. This yields a list

```
#
# warming 0.75 +- 0.125, found 137 years
#round,GCM,scenario,year
ISIMIP2b,GFDL-ESM2M,historical,1987
ISIMIP2b,GFDL-ESM2M,historical,1988
ISIMIP2b,GFDL-ESM2M,historical,1991
ISIMIP2b,GFDL-ESM2M,historical,1996
ISIMIP2b,GFDL-ESM2M,historical,1997
ISIMIP2b,GFDL-ESM2M,historical,2000
...
ISIMIP3b,UKESM1-0-LL,historical,2003
ISIMIP3b,UKESM1-0-LL,historical,2004
ISIMIP3b,UKESM1-0-LL,historical,2005
ISIMIP3b,UKESM1-0-LL,historical,2006
ISIMIP3b,UKESM1-0-LL,historical,2007
ISIMIP3b,UKESM1-0-LL,historical,2008
ISIMIP3b,UKESM1-0-LL,historical,2009
```

3. With these data we can now pick these years from the impact model runs. In case of the analysis of climate variables for WILIAM we therefore had a basis of 137 modelled years for a world at 0.75 °C global warming. Since impact models are to model all scenarios with all GCMs and scenarios this multiplies the number of available model years by the number of impact models. For instance, say there are 3 hydrological models in ISIMIP2b and ISIMIP3b (there are actually more), we would have a data base of $137 \times 3 = 411$ model years.
4. We now pick all these years from the simulation, but the data might be annual, monthly or daily, depending on the variable. In this step we condense the 365/366 daily or 12 monthly values into one annual value. How this is done exactly depends on the variable in question and is discussed in the section below. The relevant point here is that after step 4 we have a set of n (in the examples discussed in point 4. n was 137 resp. 411) global maps on a $0.5^\circ \times 0.5^\circ$ grid with one value at each grid point.
5. In this step we determine median as well as extreme values from the maps generated in step 4. Let's say that n is 411. We now sweep through each of the 720×360 grid points and get the 411 values for each of these grid points. These values are ordered from lowest to highest and we determine the 5th, 50th and 95th percentile from the set of numbers. This way we have the modelled median which is the 50th percentile as well as the low and high extreme values. The 5th and the 95th percentiles provide the baseline of extreme events to WILIAM. We picked the 5th and 95th percentile instead of the lowest and highest value to ignore extreme outliers. With this step we obtain a map of the modelled median as well as the modelled extreme values, both low and high, for a certain warming level.
6. In this step we look at the WILIAM regions. These regions are EU27, UK, CHINA, EASOC, INDIA, LATAM, RUSSIA, USMCA, LROW, AUSTRIA, BELGIUM, BULGARIA, CROATIA, CYPRUS, CZECH REPUBLIC, DENMARK, ESTONIA, FINLAND, FRANCE, GERMANY, GREECE, HUNGARY, IRELAND, ITALY, LATVIA, LITHUANIA, LUXEMBOURG, MALTA, NETHERLANDS, POLAND, PORTUGAL, ROMANIA, SLOVAKIA, SLOVENIA, SPAIN and SWEDEN. We mask out the regions for the 5th, 50th and 95th maps at each warming level and then, depending on the variable, calculate the average, the sum etc. across the WILIAM region. This way we are able to boil down the large ISIMIP data base to a number for each variable, warming level, percentile and WILIAM region. The following lines show as an example the results for the average near surface temperature (*tas*). The header states the variable and its unit. Further, the content of the columns is described. Below the header, each line gives the results for a warming level. The first entry gives the warming level, and the following entries, separated by commas, give the result for each WILIAM region.

```
#
# tas [K]
#warming, EU27, UK, CHINA, EASOC, INDIA, LATAM, RUSSIA, USMCA, LROW, AUSTRIA, BELGIUM, BULGARIA, CROATIA, CYPRUS, CZECH REPUBLIC, DENMARK, ESTONIA, FINLAND, FRANCE, GERMANY, GREECE, HUNGARY, IRELAND, ITALY, LATVIA, LITHUANIA, LUXEMBOURG, MALTA, NETHERLANDS, POLAND, PORTUGAL, ROMANIA, SLOVAKIA, SLOVENIA, SPAIN, SWEDEN
#
0.0, 281.8563896115667, 281.55050080174794, 279.9769943424149, 294.97891243154623, 297.1182150012261, 294.3347832421335, 268.04446639398736, 276.44899518446385, 291.9585333564213, 279.4196360368815, 282.85570391059116, 283.6025054981418, 284.0260776594624, 292.0222697841808, 280.897523568503, 281.0789056683313, 278.5958686437445, 274.7907469898973, 283.95005707306956, 281.8041956893877, 286.98850926721565, 283.3990968255995, 282.170635632178, 285.253022279977, 279.1350296575368, 279.6711654177292, 282.2165986747292, 291.93225066203087, 282.6742405783424, 281.0727583145145, 288.121905543958, 282.0955585796112, 280.6155924693384, 281.8208113118178, 286.45759713999416, 275.1759646036002
```

<p>0.25, 281.9844968178455, 281.7642324969992, 279.9809653350541, 295.1876348176029, 297.24611335204304, 294.5561166819599, 268.2177697163691, 276.6269913779255, 292.12047176506326, 279.55451444201526, 283.03082112061094, 283.6390910365668, 284.0631879438658, 291.9797099009833, 281.03003583310294, 281.25136731857447, 278.71479025286413, 274.9638034790238, 284.08786653321164, 281.9724804626361, 286.99431722198733, 283.4997743509254, 282.41389045189135, 285.34680320441544, 279.2304621902162, 279.7776913602342, 282.4082593345103, 291.99650400700557, 282.8298765351496, 281.1752072648151, 288.23039336338053, 282.21188343668445, 280.7498742739501, 281.89137515527983, 286.5478964233795, 275.38089124983173</p> <p>...</p> <p>4.0, 286.71404517697596, 284.7052047715278, 285.01974834467484, 298.98786445313823, 301.1981189447094, 298.6739288307606, 274.9452743612205, 282.7418694334972, 296.796178026326, 284.4559249528813, 286.799053820152, 288.7531003978876, 289.2025463834823, 295.9230145636505, 285.8203455894578, 285.1260274138422, 284.15227958346736, 281.0408222760555, 288.1897730688015, 286.271102566243, 291.66566822297665, 288.8063474340317, 284.92827221938956, 290.005129711751, 284.4983243939852, 284.91041914841566, 286.5042221233511, 295.70298782824653, 286.51759153719576, 286.04082957458223, 291.9594536736953, 287.49228944409697, 285.84232155593656, 286.9477821779126, 290.8413102675427, 280.6163319635812</p> <p>4.25, 287.0975380765433, 285.0119300302882, 285.2475781358125, 299.3636027706847, 301.49223013443003, 299.015724034244, 275.40547384805643, 283.1476024957588, 297.11906126034165, 285.02000604614614, 287.39275946105033, 288.8572973483533, 289.54004793802824, 295.93581847170657, 286.3908730093107, 285.5298550749035, 284.44906798076295, 281.39585435118215, 288.6919103023841, 286.9716918624337, 291.8430912270968, 288.975152844089, 285.0866676148852, 290.3415666901006, 284.8679802373855, 285.3385631512447, 287.16761903350374, 295.88285465831956, 286.90416628575343, 286.567378288733, 292.37305303147724, 287.6584791775737, 286.1275453392736, 287.4184041905835, 291.1263331032768, 280.925049495484</p>
--

3.4. Description of variables

The variables analysed are directly aligned with the sectors of NEVERMORE, and specifically with the sectors of WILIAM (check Deliverable 3.1 “Report on the improvements of the climate module of WILIAM” for more information (Ferrerias, et al., 2023)) for the purposes of alignment. In particular, the list is the following:

- Climate variables: aligned with the potential improvements and the downscaling of climate variables to be done in the climate module of WILIAM (Task 3.1 “Analysis of improvements and new features integration in the IAM climate module”, and Task 3.2 “Downscaling of climate information” improvements). This data can also serve as a basis for modelling extreme events.
- Crop yields: aligned with the Land module of WILIAM, which models also this variable (by type of crops) in the “Yields” submodule.
- Biodiversity: this sector or system is not yet in WILIAM, but its addition could be explored. Moreover, it is in line with the planetary boundary “Biosphere integrity” (see Section 4.3)
- Burnt areas: this can be easily related to increase of risk for fires related to climate change scenarios. This information can help to define climate risks in WILIAM. In addition, WILIAM has a Land use module, where the “burnt area” evaluation can be included.
- Evapotranspiration: This variable is part of the hydrological modules, being directly linked with the temperature (climate change impacts), as evapotranspiration increases with increasing temperature. WILIAM has a Water module where this data can be used and incorporated to deliver climate change impacts.
- Methane emissions-permafrost: this is related to the tipping point of the melting permafrost (Task 3.4 “Uncertainty assessment and tipping points of climate scenarios”).

In Table 5, a summary of the data derived from ISIMIP dataset characteristic is presented.

Table 5. Summary of NEVERMORE ISIMIP dataset.

	Name of the geospatial dataset
	<p>Median, low end (5th percentile) and high end (95th percentile) extreme values for the average, minimum and maximum near-surface temperatures, precipitation, rainfed and fully irrigated yields for corn, rice, soy and wheat, species richness for amphibians, birds and mammals, burnt areas, evapotranspiration, methane emissions and forestry NPP (The last one is still being worked on). Overall, we process 19 variables.</p>
Temporal resolution	Since the climate scenarios of ISIMIP and WILIAM are incompatible with each other we produce data in terms of global warming. The temperature resolution of this is 0.25 °C, and the warming interval runs from 0.0 °C to 4.25 °C.
Spatial Resolution	WILIAM regions (EU27, UK, CHINA, EASOC, INDIA, LATAM, RUSSIA, USMCA, LROW, AUSTRIA, BELGIUM, BULGARIA, CROATIA, CYPRUS, CZECH REPUBLIC, DENMARK, ESTONIA, FINLAND, FRANCE, GERMANY, GREECE, HUNGARY, IRELAND, ITALY, LATVIA, LITHUANIA, LUXEMBOURG, MALTA, NETHERLANDS, POLAND, PORTUGAL, ROMANIA, SLOVAKIA, SLOVENIA, SPAIN, SWEDEN).
Spatial coverage	Global, WILIAM regions (Figure 4)
Format	*.csv (comma separated values)
Use	Input for WILIAM: To include the name of the NEVERMORE product that will use this data as input. It could be an input whose use is already confirmed or a potential input that will be confirmed. Platform: if the dataset is provided directly by the platform
Source link	https://www.pik-potsdam.de/~volkholz/wiliam/csv/

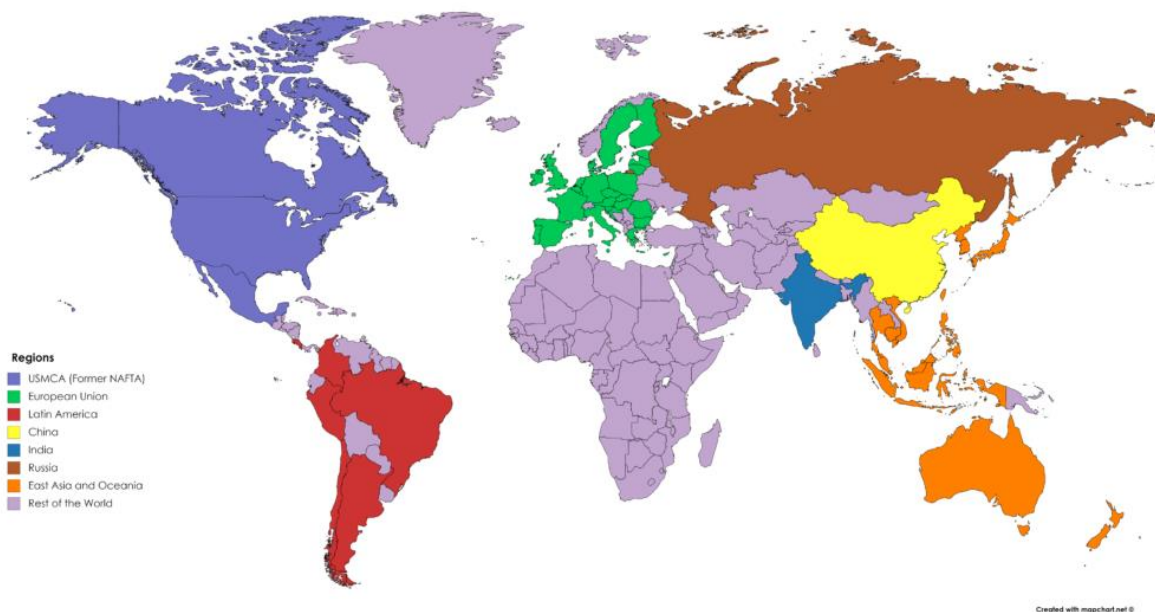


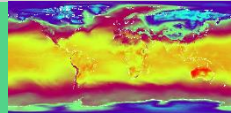
Figure 4. WILIAM regions. Source: (Pastor, et al., 2021).

3.4.1. Climate variables

The first set of variables identified in the Valladolid workshop in May 2023 were climate variables (shown in Table 6). More precisely, the WILIAM team is interested in the near-surface average temperatures (*tas*), the near-surface minimum temperatures (*tasmin*), the near-surface maximum

temperatures (*tasmax*) and precipitation (*pr*). Precipitation includes all forms of precipitation, i.e., rain, snow, and so on.

Table 6. ISIMIP climate data.

	Name of the geospatial dataset
	Near-surface average temperature (<i>tas</i>) [K], near-surface minimum temperature, (<i>tasmin</i>) [K], near-surface maximum temperature (<i>tasmax</i>) [K], precipitation (<i>pr</i>) [kg / s / m ²]
Temporal resolution	daily
Spatial Resolution	global 0.5°×0.5° grid
Spatial coverage	Global
Format	NetCDF
Use	Basis for the work in this task
Source link	https://data.isimip.org

Since the ISIMIP climate data is provided daily we had to devise algorithms to perform step 4 described in the previous section, i.e. condense 365/366 daily values to a single value. We decided on the following approach:

- *tas*: take the annual average for each grid cell [K].
- *tasmin*: take the annual minimum for each grid cell [K].
- *tasmax*: take the annual maximum for each grid cell [K].
- *pr*: sum the daily precipitation over the year [mm].

To illustrate what the results look like, we show for the case of the climate variables some results for the large WILIAM regions (Figure 5, Figure 6, Figure 7, Figure 8, Figure 9 & Figure 10). Most region tags are self-explanatory, still, some of them might warrant an explanation. In particular, we have EASOC: Southeast Asian & Oceania; LATAM: Latin America (somewhat unintuitively countries like Uruguay or Venezuela don't belong here); USMCA: USA, Mexico, Canada; LROW: rest of the world.

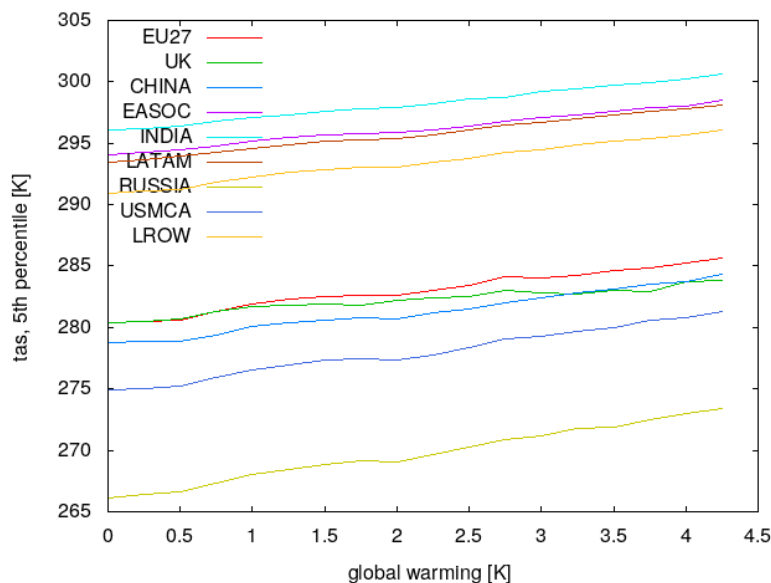


Figure 5. Low extreme values (5th percentiles) of *tas*.

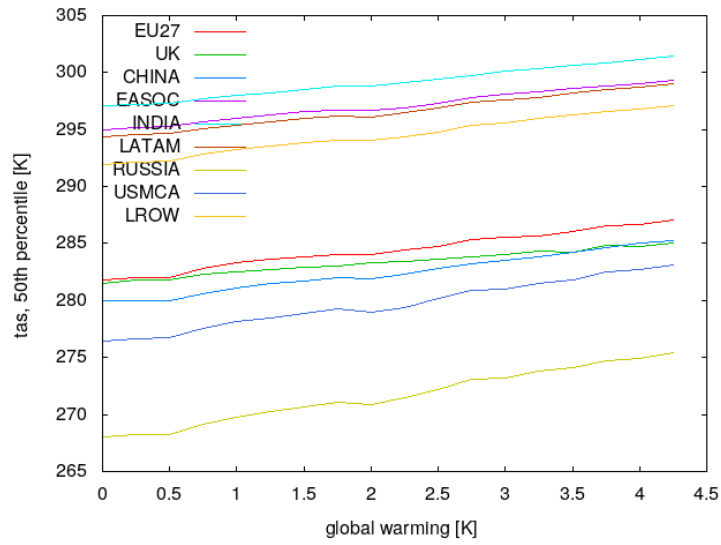


Figure 6. Median values (50th percentiles) of tas.

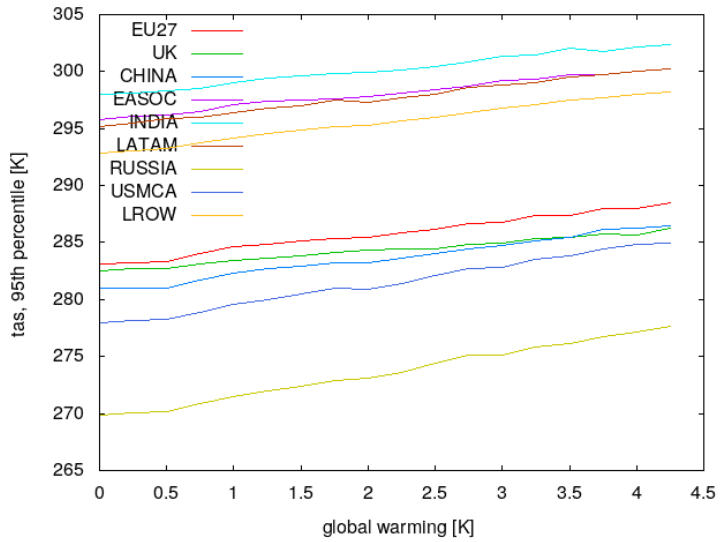


Figure 7. High extreme values (95th percentiles) of tas.

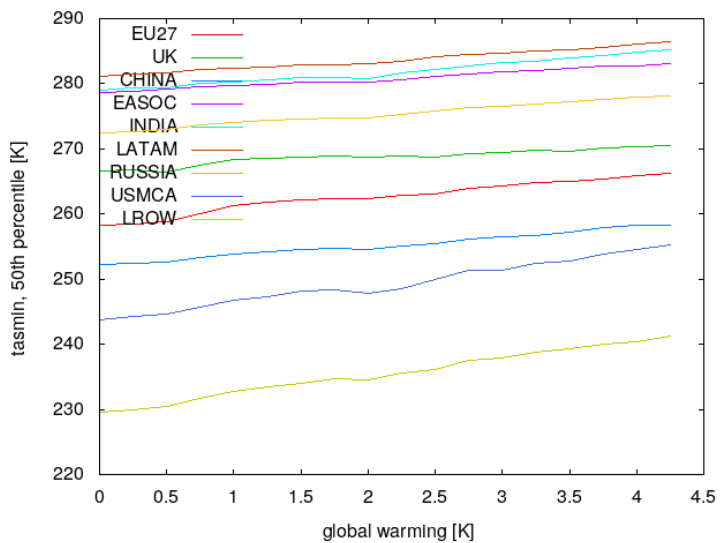


Figure 8. Median values (50th percentiles) of tasmin.

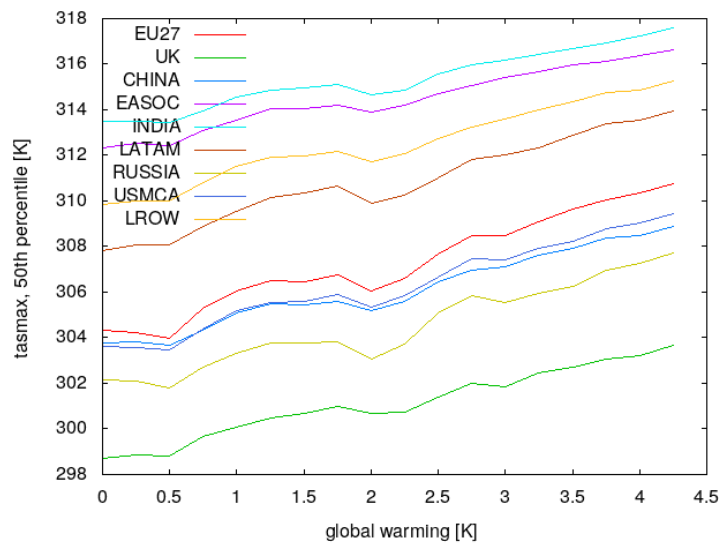


Figure 9. Median values (50th percentiles) of tasmax.

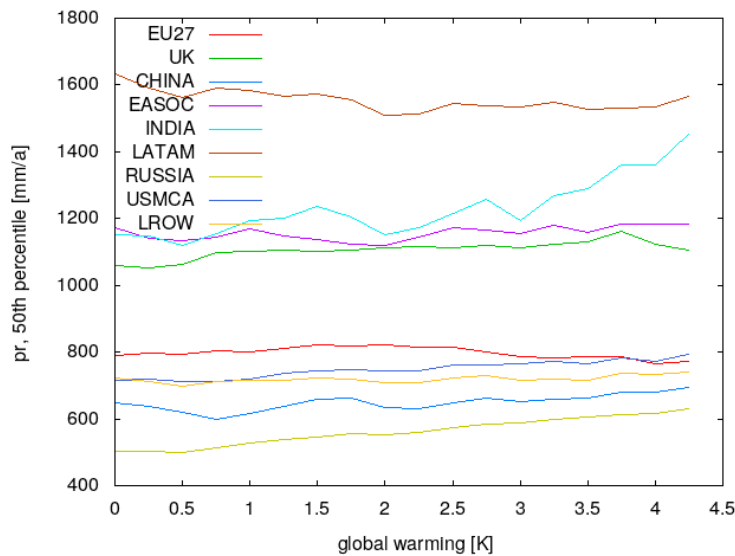
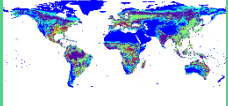


Figure 10. Median values (50th percentiles) of pr.

3.4.2. Crop yields

In ISIMIP we have a sector solely dedicated to agriculture. There are many crops included in the protocol, but globally the four major crops are corn (*mai* from maize), rice (*ric*), soy (*soy*) and wheat (*whe*) as can be observed in Table 7. The simulations in the agriculture sector in ISIMIP have a few peculiarities. One is that the models calculate potential yields. This means the crop model plants, say rice, at every point on the Earth’s land surface. Then by being driven with the climate, fertilization and, depending on the model, the CO₂ contents of the atmosphere (CO₂ fertilization effect), the yield [t/ha] is calculated. In the NEVERMORE project we are interested in “actual” yields, though. This means we only consider yields at areas where the crops are actually grown. Therefore, we have to combine the potential yield maps with landuse maps. Since, as explained earlier, the WILLIAM team is mostly interested in the climate change signal, we chose constant land use maps (ISIMIP2b: landuse fixed at 2005 conditions, ISIMIP3b: landuse fixed at 2015 conditions).

Table 7. ISIMIP crop yield data.

	Name of the geospatial dataset
	Potential crop yields [t/ha] of corn (<i>mai-nirr</i> , <i>mai-firr</i>), rice (<i>ric-noirr</i> , <i>ric-firr</i>), soy (<i>soy-noirr</i> , <i>soy-firr</i>) and wheat (<i>whe-noirr</i> , <i>whe-firr</i>). The “-noirr” and “-firr” tags refer to rainfed-only and fully irrigated
Temporal resolution	Annual
Spatial Resolution	global 0.5°×0.5° grid
Spatial coverage	Global, land surface only
Format	NetCDF
Use	Basis for the work in this task
Source link	https://data.isimip.org

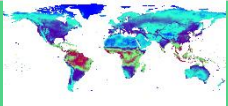
Another peculiarity of the yield variable is that modellers were required to simulate the yields twice. In one of these runs the plants obtained water only from precipitation (*noirr*) while in the other plants were fully irrigated (*firr*). The landuse maps distinguish both cases, i.e. the areas for rainfed and fully irrigated crop lands are given, so we could have combined both approaches into one yield. However, during discussions at the Valladolid workshop it was decided to keep these data separate. This leaves us with 8 variables overall: *yield-mai-noirr*, *yield-mai-firr*, *yield-ric-noirr*, *yield-ric-firr*, *yield-soy-noirr*, *yield-soy-firr*, *yield-whe-noirr* and *yield-whe-firr*.

In the case of yields we had to adapt the steps 4 to 6, the breaking down into regions had to happen before picking the percentiles. For each model year in step 3, the production (=yield × area) and the crop land area in each WILLIAM region are determined. Then we used the ratio of these (production / area) as the “actual”, as opposed to potential, yield. Subsequently, all the values obtained were ordered and the 5th, 50th and 95th percentiles were picked.

The crop yield calculations were the computationally most expensive variables. Calculating just one crop variable took up to two weeks.

3.4.3. Biodiversity

Table 8. ISIMIP biodiversity data.


	Name of the geospatial dataset
	Species richness [number of species per grid cell] of amphibians (<i>amphibiansr</i>), species richness of birds (<i>birds</i>), species richness of mammals (<i>mammalsr</i>)
Temporal resolution	Annual
Spatial Resolution	global 0.5°×0.5° grid
Spatial coverage	Global, land surface only
Format	NetCDF
Use	Basis for the work in this task
Source link	https://data.isimip.org

Currently, there are no data for biodiversity in ISIMIP3b, but ISIMIP2b had some simulation results. The variables we look at are the species richness (number of species per grid cell) for mammals (*mammalsr*), birds (*birds*) and amphibians (*amphibiansr*), shown in Table 8. We struggled a bit in step 6. The discussion was about either using, like in the case of the other variables, the field mean of the

WILIAM region, or the maximum value instead. In the end we went with the field mean, since it is a better representative of the whole region.

3.4.4. Burnt areas

Table 9. ISIMIP burnt area data.

	Name of the geospatial dataset
	Total area [percentage of grid cell] that has burned at any time (including peat and deforestation fires) (<i>burntarea/burntarea-total</i>)
Temporal resolution	Monthly
Spatial Resolution	global 0.5°×0.5° grid
Spatial coverage	Global, land surface only
Format	NetCDF
Use	Basis for the work in this task
Source link	https://data.isimip.org

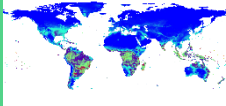
The variables for the burnt area have evolved quite a bit from ISIMIP2b to ISIMIP3b. While in ISIMIP2b there was only one variable (*burntarea*), ISIMIP3b features *burntarea-total* as well as *burntarea-<pft>*, where the *<pft>* (plant functional type) is e.g. *c4grass*. In order to be able to use data from both rounds we decided to go with the total burnt area, so we here consider any burnt vegetation such as burnt forests, burnt fields and so on. All this information is compiled in Table 9.

Another tricky point in this case is the handling of step 4, i.e. the aggregation of the sub-annual values to annual values. The ISIMIP data for burnt areas is delivered on a monthly time scale. We chose the same approach as in an earlier publication (Lange, et al., 2020). Accordingly, we assume that the burnt areas mostly don't overlap within one year, i.e. we sum the monthly burnt areas within a year. On the other hand, we assume that not more than the whole grid cell is burnt in a year, so we limit the value of the burnt area to the total area of the grid cell.

The remaining steps 5 and 6 are carried out as usual.

3.4.5. Evapotranspiration


Table 10. ISIMIP evapotranspiration data.

	Name of the geospatial dataset
	Evapotranspiration (<i>evap</i>) [kg / s / m ²]
Temporal resolution	Monthly
Spatial Resolution	global 0.5°×0.5° grid
Spatial coverage	Global, land surface only
Format	NetCDF
Use	Basis for the work in this task
Source link	https://data.isimip.org

All global hydrological models calculate evapotranspiration (*evap*) as shown in Table 10. Evapotranspiration is comprised of the water (vapour) that evaporates from water surfaces and the soil as well as the water vapour pumped into the atmosphere by the vegetation. This variable is straightforward and the steps 1 to 6 can be simply applied here.

3.4.6. Methane emissions


Table 11. ISIMIP methane emission data.

	Name of the geospatial dataset
	Total surface carbon mass flux into CH ₄ emissions (<i>ch4</i>) [kg / s / m ²]
Temporal resolution	Monthly
Spatial Resolution	global 0.5°×0.5° grid
Spatial coverage	Global, land surface only
Format	NetCDF
Use	Basis for the work in this task
Source link	https://data.isimip.org

This variable, similar to evapotranspiration, was mostly straightforward to handle. The methane emissions are interesting for WILLIAM because they are a consequence of the melting permafrost, tipping point to be analysed in Task 3.4 “Uncertainty assessment and tipping points of climate scenarios”. All the information is shown in Table 11.

3.4.7. Forestry NPP

Table 12. ISIMIP forestry NPP data.

	Name of the geospatial dataset
	Carbon mass flux out of atmosphere due to NPP on land (<i>npp-<pft></i>) [kg / s / m ²]
Temporal resolution	Monthly
Spatial Resolution	global 0.5°×0.5° grid
Spatial coverage	Global, land surface only
Format	NetCDF
Use	Basis for the work in this task
Source link	https://data.isimip.org

Both ISIMIP2b and ISIMIP3b include simulation results for NPP through several different variables such as *npp-<pft>* (as in the case of burnt areas, *<pft>* stands for plant functional type), *nppleaf-<species>*, *npproot-<species>*, *nppagwood-<species>* and *nppbgwood-<species>* (referring to leaf, root, above ground wood and below ground wood biomass, respectively). The variable to pick would be the *npp-<pft>* variables, but the implementation needs further analysis. All the information is shown in Table 12.

3.5. Downscaling method for ISIMIP data

As part of the harmonization of the outcomes of the climate, impact and risk information across different scales, we attempt to downscale the gridded information of some of ISIMIP variables to a higher resolution, to be more useful for local case analysis. The approach is based on the AI downscale approach that is developed in Task 3.2 “Downscaling of climate information” and it utilizes external evidence in order to successfully downscale climate variables, such as, temperature.

More specifically, the option of using Convolutional Autoencoders (CAEs) with evidence transfer is explored in the case of ISIMIP gridded data as well. CAEs are a combination of Convolutional Neural Networks (CNNs) and Autoencoders and they utilize convolutional layers for encoding and decoding and are well-suited for image processing due to their ability to exploit image structure. The CNNs are specialized for processing grid-like data, such as images, and employ convolution operations to extract features. They leverage ideas like sparse interactions, parameter sharing, and equivariant representations, making them effective for image and audio signal processing. On the other hand, autoencoders are neural networks that learn to copy their input to their output and can be categorized into various types, including undercomplete, overcomplete, regularized, sparse, and denoising autoencoders. They find applications in dimensionality reduction, feature learning, and generative modelling.

In the context of evidence transfer, a pre-trained CAE can be used to integrate external evidence, such as season, climate variables, landuse, etc. into the task of reconstruction. This process involves initialization, evidence preparation, and input evidence steps, ultimately adjusting the latent space weights. Evidence transfer enhances the performance of CAEs in tasks like dynamic error correction in downscaling gridded data (Karozis et al., 2023).

The method is going to be tested with ISIMIP data and explore the option of providing higher resolution impact datasets to be used from local actors in risk assessment and adaptation to climate change.

4. Planetary boundaries

One of the objectives of this deliverable is to provide a methodology to include planetary boundaries in WILIAM. WILIAM is an integrated assessment model (IAM) with a high level of disaggregation and non-linear relationships (see NEVERMORE Deliverable 3.1 (Ferrerias, et al., 2023)) for a further description of the WILIAM IAM). This section aims to provide a framework for the evaluation of the so-called planetary boundaries, focusing on the key aspects that will be considered for their subsequent incorporation and modelling in the WILIAM model. This integration in WILIAM will be done in the subsequent years of the project and incorporated in the updated versions corresponding to the Task 4.5 “Integration in the IAM considering future feedbacks and cascading effects and validation”. For the time being, the ideas explained here should serve to set some methodological guidelines that support the modelling, that will be refined in the scope of Task 4.5.

The planetary boundaries are a global environmental sustainability framework for identifying critical transitions or tipping points in the complex Earth System, based on control and response variables (Gleeson, et al., 2020). A more detailed definition of the main aspects involved in this framework is provided in Section 4.1. Section 4.2 provides a description of the meaning of each planetary boundary and the control variables that are often used in the literature to assess the safety space for humanity. Section 4.3 briefly identifies which planetary boundaries can be modelled, based on their alignment with the methodology proposed in the Deliverable 3.1 (Ferrerias, et al., 2023) and the current attributes of WILIAM. Also, modelling options for the control variables of some planetary boundaries are proposed.

A summary table (Table 13) of each planetary boundary with their related control variables and the most widely used values in the literature is provided at the end.

4.1. Introduction into planetary boundaries

Planetary boundaries define the safe operating space for humanity with respect to the Earth System and are associated with the planet's biophysical subsystems or processes (Rockström, et al., 2009) that regulate the stability of the Earth System (Steffen, et al., 2015). Although Earth's complex systems sometimes respond smoothly, many subsystems of the Earth react in a nonlinear, often abrupt, way, and are particularly sensitive around threshold levels of certain key variables. If these thresholds are crossed, then important subsystems could shift into a new state, often with deleterious or potentially even disastrous consequences for humans. Thresholds are intrinsic features of those systems (Rockström, et al., 2009) and can be defined by a critical value for one or more control variables, such as carbon dioxide concentration. However, not all processes or subsystems on Earth have well-defined thresholds (Rockström, et al., 2009).

It is also important to emphasize the difference between a planetary boundary and a tipping point. The IPCC defines tipping points as “critical thresholds in a system that, when exceeded, can lead to a significant change in the state of the system, often with an understanding that the change is irreversible” (IPCC, 2022). The definition refers to the fact that if certain resilience variables (in this framework, control variables) in the earth system cross a threshold, the response of the system may be abrupt, non-linear and irreversible. The potential nonlinear response (tipping point) that may result from the deterioration of the resilience variables of the earth system due to the crossing of certain thresholds of these variables is not studied in the framework of this assessment. Some authors emphasize this difference between planetary boundary and tipping point: “A planetary boundary as originally defined is not equivalent to a global threshold or tipping point. As Figure 10 shows, even when a global- or continental/ocean basin–level threshold in an Earth-system process is likely to exist, the proposed planetary boundary is not placed at the position of the biophysical threshold but rather upstream of it—i.e., well before reaching the threshold” (Steffen et al., (2015, pp2)). Frequently, the planetary boundary assessment framework is used to identify critical transitions or tipping points in the complex earth system, based on control and response variables (Gleeson, et al., 2020). So, the planetary boundaries may warn us, precisely, of the occurrence of a tipping point on earth.

For the integration of the planetary boundary concept in WILIAM, it is worth mentioning that we are not going to model the “response variable” in Figure 11, but the control variable on the x-axis of this same figure, which will indicate how close we are to exceeding limits beyond which the response of the Earth System can be nonlinear, abrupt and destructive. Based on the above definition, there are some key concepts that must be defined and quantified within the framework of this evaluation.

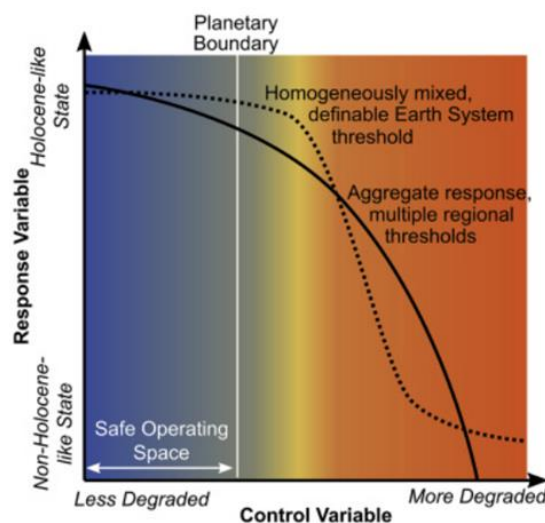


Figure 11. Planetary Boundary Framework, showing two of the many potential types of relationships between a control and response variable. Source: (Gleeson, et al., 2020).

- **Selected planetary boundaries:** The planetary boundaries selected in this assessment are derived from Rockström et al. (2009) who identify nine thresholds above which the Earth system processes change abruptly or nonlinearly. However, the evolution of the control variables can be linear or not, and despite their evolution, they could generate a non-linear response in the Earth System. However, other authors suggest including new planetary boundaries not considered by this original study, as is the case of green water (terrestrial precipitation, evaporation and soil moisture) which is also a process associated with a planetary boundary (Wang-Erlandsson, et al., 2022).
- **Quantification of the threshold uncertainty band:** Steffen et al. (2015, pp3) affirm that the band of uncertainty *“not only accounts for uncertainty in the precise position of the threshold with respect to the control variable but also allows society time to react to early warning signs that it may be approaching a threshold and consequent abrupt or risky change”*. Therefore, the uncertainty band is quantified considering scientific uncertainty about certain terrestrial processes and leaving a time margin for reaction. Usually, in all papers, the planetary threshold value is associated with an uncertainty band.
 It should be noted that some of the values provided in this section to quantify the uncertainty band correspond to the concept of "zone of increasing risk", because they quantify more than the scientific uncertainty itself. The values associated with this concept (zone of increasing risk) are those from the reference (Richardson, et al., 2023). More information on the subject can be found in Richardson et al. (2023). However, "uncertainty band" and "zone of increasing risk" values will be used interchangeably (being aware that they are not the same) when necessary due to lack of data.
- **Value of thresholds:** Despite the above definition, "threshold" (as a single value) is defined, following the principle of caution, as the lower limit of the uncertainty band, considering that *“each proposed boundary position assumes that no other boundaries are transgressed”* (Rockström, et al., 2009). In addition, it is necessary to indicate the scale on which the values of the thresholds are given. Some studies make a global and aggregated analysis, in which they consider the control variables at the planetary level and review whether boundaries have been crossed on a planetary rather than regional scale. However, Steffen et al. (2015, pp3) caution that *“changes in control variables at the subglobal level can influence functioning at the Earth-system level, which indicates the need to define subglobal (regional) boundaries that are compatible with the global-level boundary definition. Avoiding the transgression of subglobal boundaries would thus contribute to an aggregate outcome within a planetary-level safe operating space”*. The Holocene is taken as the reference for the value of the planetary boundary thresholds.
- **Selection of control variables:** The control variables proposed in Rockström et al (2009) are used; however, other control variables proposed by other studies are also considered.
- **Feedback between planetary boundaries:** In the framework of this evaluation, the numerical value of a threshold (associated with a planetary boundary) does not change if another planetary boundary is exceeded, which is a simplification of reality (Rockström, et al., 2009). Furthermore, this analysis does not consider, in principle, connections between planetary boundaries: these connections would cause the value of the thresholds to change and could even influence the value of the control variables themselves (Lade, et al., 2019). Since the integrated assessment model (WILIAM) is being used, it is possible to analyse, based on the structure of the model itself, how the control variables that define some planetary boundaries affect others (although, as has been emphasized, not all the interconnections between planetary boundaries have been explicitly modelled). This fact should not be overlooked and should be treated with caution since the effect of feedbacks between planetary boundaries tends to bring the control variables closer to the high-risk zone. Lade et al. (2019) quantify the

direct effect of humans on the control variables and the indirect effect due to feedbacks between planetary boundaries.

4.2. Description of the planetary boundaries

This section explains each planetary boundary, along with an overview of the typical control variables utilized in the literature to evaluate humanity's safety zone. In some cases, we also suggest additional control variables and quantitative thresholds that can be useful for their integration in WILIAM.

- **Climate Change**

The evaluation framework for this planetary boundary will use the definition given by Rockström et al. (2009, pp9) which states: “*The climate-change boundary proposed here aims at minimizing the risk of highly non-linear, possibly abrupt and irreversible Earth System responses related to one or more thresholds, the crossing of which could lead to the disruption of regional climate*”. The key to this planetary boundary, as Rockström et al. (2009) explains, is that the climate model that analyses it needs to be designed to capture long-term shifts in weather patterns and feedbacks to adequately represent the long-term future impact given a concentration of greenhouse gases.

Rockström et al (2009) suggest atmospheric CO₂ concentration and radiative forcing as global-scale control variables. Other widely used variables are the global average temperature increase, for which there is a defined limit of 1.5°C according to the Paris Agreement (however, this value exceeds the risk zone proposed in recent papers such as in Richardson et al. (2023)). At the regional level, the average temperature increase could also be used, but it would be necessary to find thresholds at this scale that are consistent with the proposed global thresholds, which could increase modelling difficulty.

- **Ocean Acidification**

This planetary boundary is closely related to the preservation of marine biodiversity (related to the integrity of the biosphere which is another planetary boundary) and the consequences of species extinction for the food chain and other organisms.

The concentration of free H⁺ ions in the surface ocean has increased by about 30% (which is equivalent to a 30% decrease in pH, which means going from pH 8.2 to 8.1) over the past 200 years due to the increase in atmospheric CO₂. This, in turn, influences carbonate chemistry in surface ocean waters. Specifically, it lowers the saturation state of aragonite, CaCO₃ (the planetary threshold of 80% in Table 13 refers to the concentration of this mineral) (Steffen, et al., 2015). This mineral is necessary for the formation of the shells of many marine species as well as for the organism of corals. Moreover, as the concentration of this mineral decreases and the acidity of the ocean increases, aragonite shells are expected to dissolve (Rockström, et al., 2009).

The control variable officially proposed by the original study was the concentration of aragonite in the oceans (Ω_{arag}) compared to the pre-industrial era on a global scale (Rockström, et al., 2009), but updated literature also studies the loss of marine biodiversity in terms of pH, as in Bednaršek et al. (2021) where different thresholds are proposed, beyond which the vital processes of marine decapods begin to be compromised.

- **Biogeochemical flows**

This phenomenon consists of the modification of the nutrient cycles, mainly nitrogen (N) and phosphorous (P), due to anthropogenic activities, in particular agriculture and industry, but also domestic tasks. Human-induced releases of the highly reactive forms of these elements can severely affect terrestrial and marine ecosystems. However, the planetary boundary framework mentioned above just quantifies the concentrations of nutrients in water systems, differentiating between N and P.

Regarding the phosphorous cycle, there are two accepted indicators: (a) a global indicator originally proposed by Rockström et al. (2009) which seeks to avoid the appearance of anoxic oceans; and (b) a novel, regional indicator based on studies by Carpenter & Bennet (2011) that aims to prevent the eutrophication of freshwater systems.

- (a) Global indicator: It refers to the P flow from freshwater systems to oceans (control variable) with a proposed limit of 11 Tg P/yr. This indicator is the most likely to be implemented in the model since it includes emissions from several sources, not only from croplands.
- (b) Regional indicator: It just considers P discharges from fertilizers to croplands (which then end up in freshwater), with a boundary of 6.2 Tg P/yr.

For nitrogen, unlike phosphorous, there is only one indicator, and it has a global perspective. The control variable is the industrial and intentional fixation of N with a limit of around 62 Tg N/yr. This boundary has a high uncertainty since most emissions come from agriculture (fertilizers), whose data are not well validated (de Vries et al., 2013).

- **Stratospheric ozone depletion**

This planetary boundary refers to the thinning of the ozone layer inside the Polar Regions, but also outside them, caused by ozone depleting substances (ODS).

As specified in Rockström et al. (2009, pp7), *“In the case of global, extra-polar stratospheric ozone, there is no clear threshold around which to construct a boundary. As such, the placement of our boundary in this case is of necessity more uncertain than, for example, in the case of ocean acidification. We consider the planetary boundary for ozone levels to be a <5% decrease in column ozone levels for any particular latitude with respect to 1964–1980 values”*.

The originally proposed control variable (O₃ concentration) is quite complicated to model, therefore many models, e.g. MAGICC (Meinshausen et al., 2011) or CICERO-SCM (Skeie et al., 2017), directly calculate the impact of the concentration of ODS gases on the ozone layer using the concept of EESC (Equivalent Effective Stratospheric Chlorine) (Newman, et al., 2007). This indicator is a metric to represent ODS levels in the stratosphere, so that if the EESC increases, the ozone layer degradation also increases, with an officially accepted threshold of 3 ppb EESC in the atmosphere (WMO, 2022).

- **Atmospheric aerosol loading**

Aerosols are particles emitted using fossil or biogenic fuels that influence various aspects such as: human health, albedo coefficient, radiative forcing, the hydrological water cycle, etc.

The suggested control variable in the original article is AOD (Aerosol Optical Depth) that is a quantitative estimate of the amount of aerosol present in the atmosphere. It is dimensionless and ranges from 0 to 1. Reaching the maximum value would mean that the atmosphere, in that particular region and time, is completely opaque to the penetration of light. Steffen et al. (2015) suggest setting the threshold at 0.25 AOD but treating this value with caution due to its uncertainty.

- **Land System Change**

Steffen et al. (2015) propose a new control variable (alternative to the original which was "amount of cropland") with the objective of studying how the degradation of the three most important forest biomes (tropical, temperate and boreal) affects the development of the earth system, understanding that these play a more important role in land surface-climate coupling. Measuring the safe operating space (planetary boundaries) of global forests is essential to determine global forest pressure and manage forests sustainably (Zhang, et al., 2021).

The threshold of the originally proposed control variable (percentage of covered land converted to cropland) was set at ≤15% of the global ice-free land surface converted to cropland (15%-20%) (Rockström, et al., 2009). The proposed global thresholds for the new control variable (amount of forest cover remaining by forest type: tropical, temperate and boreal) has been set to 85% for tropical

and boreal forests and 50% for temperate forests. Alternatively, Zhang et al. (2021, pp4) propose as a control variable the forest stock increment so that *“the higher the forest stock increment, the higher the safe operating space for human harvesting. In contrast, a lower forest stock increment implies a higher boundary-exceeding risk.”* The study focuses on the relationship between human logging activities and the safe operating space for harvesting and establishes specific regional thresholds, which are shown in Figure 12.

a National forestry boundaries (million m³)

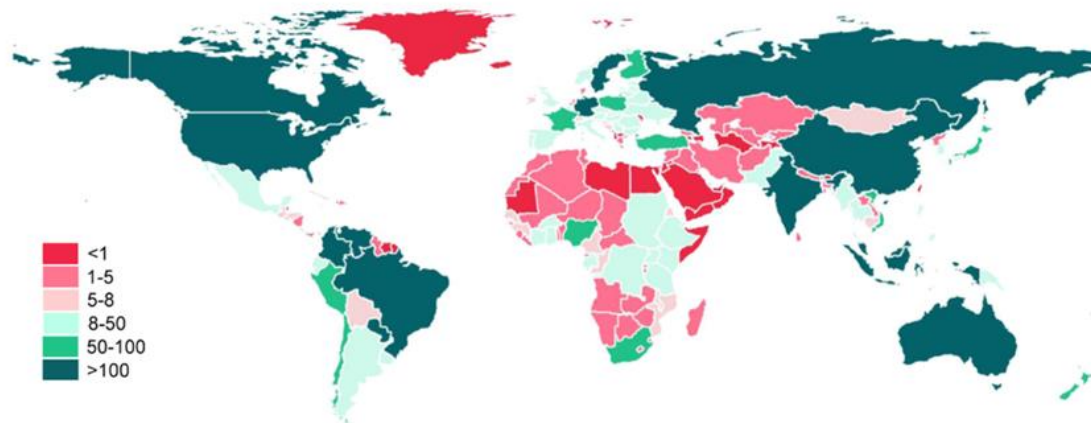


Figure 12. Average forestry boundaries of nations during 1991–2015. Source: (Zhang et al., 2021)

- **Freshwater use**

This planetary boundary is based on allowable human blue water consumptive use. The control variable that typically represents this planetary boundary is the use of blue water at the global level (from rivers, lakes, reservoirs, and renewable groundwater stores). The threshold was originally set at 4000 km³/yr (Rockström, et al., 2009). Other studies have proposed to study this planetary boundary with monthly time scale indicators (as the variable monthly flow (VMF)), which does not agree with the time scale at which WILIAM computes. However, this control variable suffers from some limitations since it studies this phenomenon in an aggregate form without distinction between blue water (freshwater flow) and green water (water in vegetation or soil moisture). Richardson et al. (2023) propose a different global threshold for each of the above-mentioned classes and instead suggest as control variable the percentage of annual global ice-free land area with streamflow/rootzone soil moisture deviations from preindustrial variability. Although the control variable is annual, the study analyses the impact on a monthly scale in order to later construct an annual indicator. In principle, this is not possible in WILIAM, as mentioned before.

It is important to understand that the hydrosphere theoretically includes five types of water stores: surface water, soil moisture, atmospheric water, groundwater and frozen water (as illustrated in Figure 13). Therefore, it must be determined whether the global threshold studies the impact on all stores or only on one or some of them. Currently, the most common approach is to assess the impact on surface water and soil moisture.

The diagrams of the figure, show the five stores of the freshwater hydrosphere (coloured circles in centre), major components of the Earth System (outer ring), and detailed Earth System components underlying the different planetary boundaries (inner grey ring). The arrows denote the processes linking the water stores and the Earth System components.

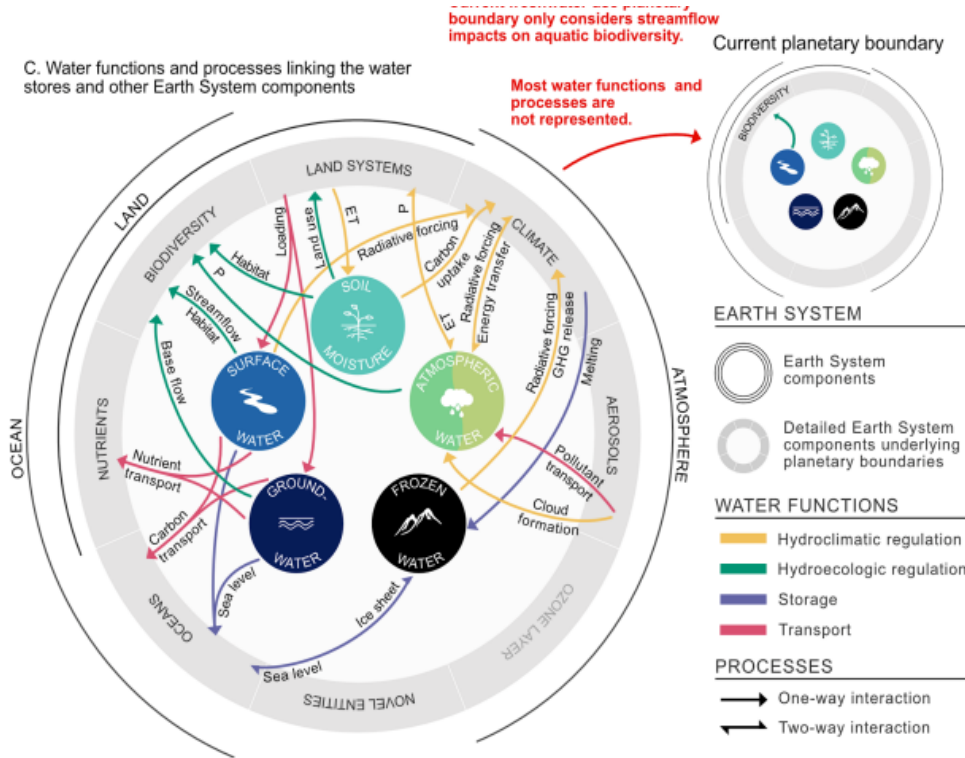


Figure 13. The core functions of water in the Earth System (larger diagram) and how they are represented in the current freshwater use planetary boundary (small diagram). Source: (Gleeson, et al., 2020).

- **Novel entities**

This planetary boundary refers to the introduction of anthropogenic chemicals into the Earth's system. (Richardson et al. (2023, pp2) specifies: "These include synthetic chemicals and substances (e.g., microplastics, endocrine disruptors, and organic pollutants); anthropogenically mobilized radioactive materials, including nuclear waste and nuclear weapons; and human modification of evolution, genetically modified organisms and other direct human interventions in evolutionary processes". In general, there is no clear threshold accepted by the current literature, although some authors believe that this planetary boundary has already been transgressed (Richardson, et al., 2023). More information on this issue is provided in the following section.

- **Biosphere integrity**

The planetary functioning of the biosphere ultimately rests on its genetic diversity. Genetic diversity and planetary function, each measured through suitable proxies, are therefore the two dimensions that form the basis of a planetary boundary for biosphere integrity (Richardson, et al., 2023).

In the literature, several authors like Steffen et al. (2015) or Rockström et al. (2009) have discussed the suitability of different control variables to capture the impact of humans on the integrity of the biosphere, according to the previous definition. The control variables proposed by these authors (e.g. extinctions per million species-years E/MSY or Biodiversity Intactness Index BII) are often complicated to compute in models. For this reason, Richardson et al. (2023) propose an alternative indicator: the NPP (Net Primary Production). The planetary limit proposed for this variable is the limit to the human appropriation of the biosphere's NPP (HANPP) as a fraction of its Holocene NPP. NPP is essential for human society but also for biomes to maintain their ecological functions, which is why the two ecosystems are in competition. For this reason, it is necessary to measure the flow of energy associated with NPP that humans deviate for their own consumption in detriment of the biosphere's integrity.

It is important to point out that “HANPP designates both the harvesting and the elimination or alteration (mostly reduction) of potential natural NPP, mainly through agriculture, silviculture, and grazing” and that will be measured with respect to the mean NPP during the Holocene, although there are other references (Richardson et al. (2023, pp4)). Therefore, the global threshold established by Richardson et al. (2023) for the NPP that will be used in this assessment framework is 55.9 Gt of C/yr \pm 1.1 Gt of C/yr.

4.3. Current status at WILIAM and modelling proposals for each planetary boundary

This section analyses the modelling feasibility of each planetary boundary according to the current state of the WILIAM model. It proposes potential modelling solutions for some planetary boundaries based on the existing variables in the IAM and the possible improvements that are contemplated in other tasks of this project. The methodology presented here is complementary to the one presented in Deliverable 3.1 (Ferrerias, et al., 2023), which can be used to expand on certain concepts and developments.

- **Climate change**

With data from the climate module of the WILIAM model (see Deliverable 3.1 for more information (Ferrerias, et al., 2023)) it is possible to analyse the two control variables originally proposed (atmospheric CO₂ concentration and radiative forcing) on a global scale, as well as to evaluate the other alternative control variables (global and regional mean temperature increase) that contribute to the assessment of the risk status of this planetary boundary. See Table 13 for specific information on threshold values and their uncertainty.

- **Ocean acidification**

Currently, the WILIAM model calculates in detail the variable increase of pH in the oceans, mainly based on the increase of atmospheric CO₂. Following the methodology described in Deliverable 3.1 (Section 6.1.1.1.3 Ocean acidification) (Ferrerias, et al., 2023), the aragonite saturation is calculated. In this way, the potential transgression of this planetary boundary can be studied in terms of pH or CaCO₃ concentration. Furthermore, this planetary threshold is also related to the planetary boundary of climate change, so that the 80% threshold would not be transgressed if the climate change threshold of 350 ppm CO₂ is respected (Steffen, et al., 2015).

- **Biogeochemical flows**

At present, biogeochemical cycles are not included in WILIAM in any form, so their implementation must be carried out basing the efforts on compiling information from literature as well as other SDMs. The methodology for this task has been exhaustively described in Deliverable 3.1 (Sections 5.2.2 and 6.1.1.1 Biogeochemical cycles) (Ferrerias, et al., 2023) and it is inspired by the submodule “Nutrient Cycles” of the ANEMI model (Breach & Simonovic, 2021). Whereas nitrogen and phosphorous anthropogenic sources are very similar, the representation of their cycles differs, since only nitrogen incorporates an atmospheric component.

Agricultural activities, which are primarily responsible for this type of pollution, release nutrients through leaching of fertilizers, which end up in rivers and reservoirs. Industries and households also generate a relevant share of emissions through wastewater streams that can be treated, untreated or reused flows (each one with a different nutrient concentration). The Nitrogen fixation threshold, whose value is 62 Tg N/yr, is to be modelled using a proxy called “Wastewater input” which is calculated as the sum of the emissions released by the sectors mentioned above.

As was discussed in the previous section, the global phosphorous limit (11 Tg P/yr) has been chosen over the regional one. Thus, it is to be derived from a variable in the ANEMI model which represents the flux from coastal waters to ocean surface (Carpenter & Bennett, 2011; de Vries et al., 2013).

- **Stratospheric ozone depletion**

The inclusion of this planetary boundary in the WILLIAM model requires specific modelling of the atmospheric concentration of ozone depletion precursor gases, which would lead to a substantial improvement of the model's climate module. The calculation of this planetary boundary is in line with the methodology presented in Deliverable 3.1 (Section 6.1.1.2 Stratospheric Ozone Depletion) (Ferreras, et al., 2023), where the radiative forcing due to ozone layer degradation is to be calculated. For the estimation of the radiative forcing it is necessary to previously calculate the EESC that will also serve as an alternative control variable to analyse the state of this planetary boundary. A value of 3 is taken as a threshold (WMO, 2022).

- **Atmospheric aerosol loading**

Streets et al. (2009) calculates the annual AOD for different regions from 1980 to 2006 by first establishing a relationship between emissions of different aerosols (BC, OC, Sea Salt, Sulfur and Dust) and the AOD for the year 2001 using the GOCART and MATCH model. Their study covers a short period of time and therefore they assume this 2001 emissions-AOD relationship to be constant for the entire study range. If a longer-term study were to be done, it is possible that other types of data would have to be searched for. Equation 5 shows the typical relationship between AOD and aerosol emissions.

$$AOD_{j,i,t} = f_{j,i} \cdot Em_{j,i,t}$$

Equation 5

Where j , i and t are the species, regions and year respectively, Em the emissions and f the modelled parameter for 2001. The modelled parameter f can be obtained from the data in Figure 14.

Region	Parameter ^b	Sulfur	BC	OC	Sea Salt	Dust
United States	Emissions	8.05	0.36	1.62	11.67	8.24
	Total mass burden	0.03	0.00	0.02	0.07	0.61
	AOD	0.07	0.00	0.01	0.00	0.03
South America	Emissions	2.25	0.27	2.00	43.46	20.43
	Total mass burden	0.01	0.00	0.03	0.10	0.13
	AOD	0.04	0.00	0.02	0.01	0.01
OECD Europe	Emissions	6.02	0.30	0.50	27.03	0.00
	Total mass burden	0.02	0.00	0.01	0.10	0.41
	AOD	0.10	0.01	0.01	0.02	0.05
Russia	Emissions	3.99	0.19	0.97	0.20	0.00
	Total mass burden	0.02	0.00	0.01	0.05	0.63
	AOD	0.14	0.01	0.02	0.01	0.06
Southern Africa	Emissions	2.55	1.40	1.14	28.71	17.73
	Total mass burden	0.02	0.02	0.13	0.09	0.12
	AOD	0.04	0.02	0.07	0.01	0.01
South Asia	Emissions	3.33	0.55	1.93	14.21	16.36
	Total mass burden	0.01	0.01	0.02	0.05	0.59
	AOD	0.08	0.01	0.03	0.01	0.06
East Asia	Emissions	16.16	1.72	4.43	18.29	281.2
	Total mass burden	0.08	0.02	0.06	0.31	3.84
	AOD	0.11	0.01	0.02	0.01	0.08
Southeast Asia	Emissions	2.48	0.59	3.46	56.00	0.00
	Total mass burden	0.02	0.01	0.04	0.13	0.12
	AOD	0.05	0.01	0.02	0.01	0.01

^aResults for Sulfur, BC, OC, and sea salt are from the GOCART model. Results for dust are from the MATCH model, as described in the text.

^bEmissions are given in Tg M/a, and total mass burden is given in Tg M.

Figure 14. Emissions, Total Mass Burden and AOD by Region for 2001. Source: (Streets, et al., 2009).

With data provided in Streets et al. (2009), only aerosols of BC, OC and sulfur would be covered, so data for NH₃ would be missing. The study in Figure 15 provides other values of the factor “ f ”, the image shows the AOD - aerosol emissions relationship proposed by Chin et al. (2014) for some

regions of the world (United States, Europe, East Asia and South Asia), the equation is shown in the image in blue for three aerosol species (OC, BC and sulphur, again missing NH₃). OM is organic matter and typically corresponds to OM = OC * f where f = 1.4 - 2.2 in the literature.

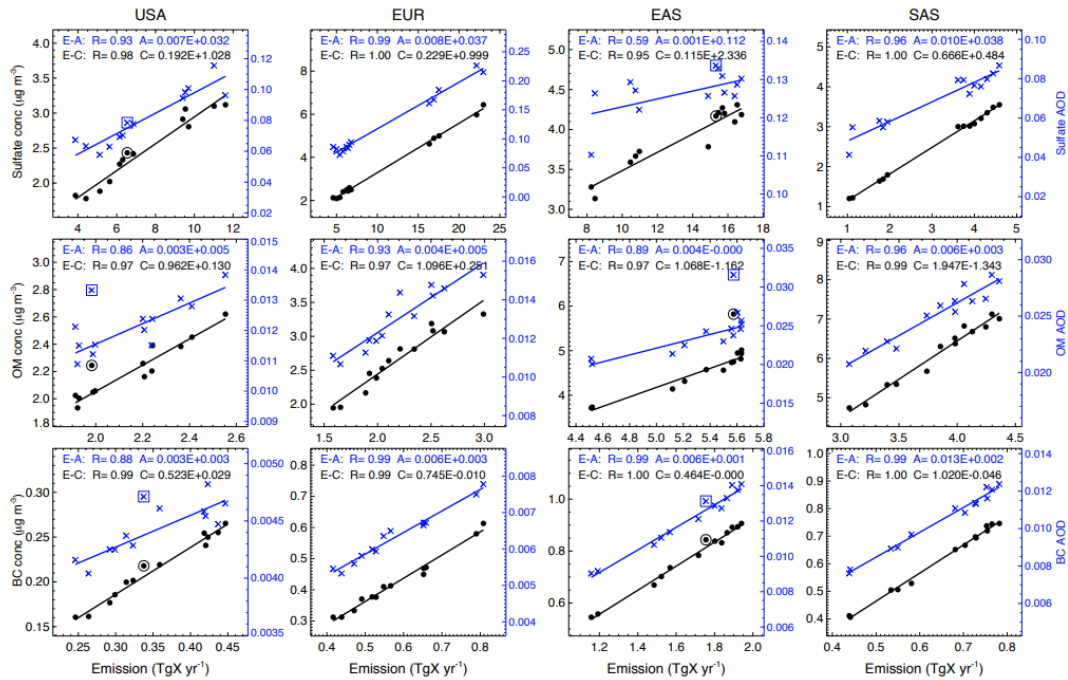


Figure 15. Model estimated relationship between emission (E) and surface concentrations (C) (black dots) or AOD (A) (blue crosses) of SO₂, OM and BC on regional and annual average over different regions. Source: (Chin, et al., 2014)

This way, the control variable could be estimated endogenously on a regional scale, having previously computed the emissions of each aerosol species (how to model the emissions of each type of aerosol is discussed in other tasks of this project, (see Deliverable 3.1, Section 5.2.6 “Tropospheric aerosol direct radiative forcing” (Ferreras, et al., 2023)). The methodology to be explored to endogenize the emissions of each aerosol species in the WILIAM model is explained hereafter.

We would like to relate the emissions of each aerosol species to the activity of each WILIAM sector (depending, for example, on its primary energy consumption which would serve as a driver) or to each WILIAM region (depending on the complications of the data search). To achieve this, we consider the so-called Emission Factors (EF). This concept is widely used to estimate emissions associated with an activity; the EPA (United States Environmental Protection Agency) defines this parameter as “a representative value that attempts to relate the quantity of a pollutant released to the atmosphere with an activity associated with the release of that pollutant. These factors are usually expressed as the weight of pollutant divided by a unit weight, volume, distance, or duration of the activity emitting the pollutant (e.g., kilograms of particulate emitted per megagram of coal burned)”. In the simplest form, the EF is defined by Equation 6:

$$Em_j = EF_{j,s} \cdot Driver_{i,s}$$

Equation 6

Where Em is the emission of a given aerosol j [Kg], EF is the emission factor associated with a sector s (or region) and a species j [kg of aerosol emitted/GJ of energy consumed by the sector or region] and the Driver is, in general, the primary energy consumed by the sector or region to which these emissions are associated [GJ]. However, other drivers could be considered.

Nevertheless, this definition involves using controlled EFs, which include in their own estimation the emission reduction efficiency and assume it to be constant over time. A more general definition would

be the one provided by the EPA Equation 7 where the emission factor is not controlled and therefore, efficiency is considered as a separate parameter (ER).

$$Em_j = EF'_{j,s} \cdot Driver_{i,s} \cdot (1 - (ER_s)/100)$$

Equation 7

Where EF' is the uncontrolled emission factor and ER is the emission efficiency of a given technology or sector, which can be constant or time-varying.

The complications involved in the use of emission factors are the lack of estimates in the current literature of EFs for each sector or WILIAM region and the uncertainty itself associated with the calculation of these EFs, as their value often changes quite a bit from one study to another.

An alternative methodology to be explored will be the calculation of emission factors based on data from the WILIAM energy module and data from the EDGAR aerosol emissions database.

Once the appropriate emission factors for the WILIAM characteristics have been calculated or obtained from a literature review, Equation 5 could be used to estimate the AOD with the data in Figure 14, or other similar data. The calculation of the AOD indicator, however, is not free of uncertainty because this parameter strongly depends on the specific atmospheric conditions of each region.

- **Land system change**

The WILIAM model currently contains a land use module that specifically describes forest growth and timber use. The model is designed to differentiate by forest type, including primary, managed and plantation. The current structure of the model itself does not allow for the study of the control variables proposed in this section on the scale proposed by the authors cited above. Possible modifications will be evaluated to calculate the mentioned variables by forest type (temperate, boreal and tropical). However, with the current structure it is theoretically possible to study the control variable, forest stock increment, in aggregate global terms.

- **Freshwater use**

The most feasible way to analyse this planetary boundary is to use data from WILIAM to study freshwater consumption, a control variable proposed by Rockström et al. (2009). However, it would not include the entire planetary boundary, but only a part of it, as we have already emphasized. To do that, the first step would be to modify the model to discriminate between green water and blue water demand, which are currently computed on an aggregate basis. An advantage of WILIAM is that this variable can be examined at both the regional and global levels. It is also possible to evaluate the water demand of each sector represented in the model. Nonetheless, other control variables will be explored depending on the data availability and modeling feasibility according to the characteristics of WILIAM.

ISIMIP provides a repository of evapotranspiration and precipitation data that are used for improvements in the WILIAM climate module, see Sections 3.4.5 and 0, and to represent some of the functions illustrated in Figure 13.

- **Novel entities**

This planetary boundary is still largely unexplored (Rockström, et al., 2009; Steffen et al., 2015; Richardson et al., 2023), which makes its modelling extremely complicated. Moreover, at present, there is no clear threshold for this planetary boundary in the literature, nor is there consensus on a specific control variable (Persson, et al., 2022).

- **Biosphere integrity**

Currently, the WILIAM model has a landuse module that defines, as mentioned above, the growth of forests (affected by land use change for other purposes); the NPP variable is modelled in this module.

With some adaptations to match the definition proposed by Richardson et al. (2023) (illustrated in Figure 16) and to preserve the consistency of the analysis, the transgression of this planetary boundary could be studied. For more information about the specific reference values of this threshold see Table 13.

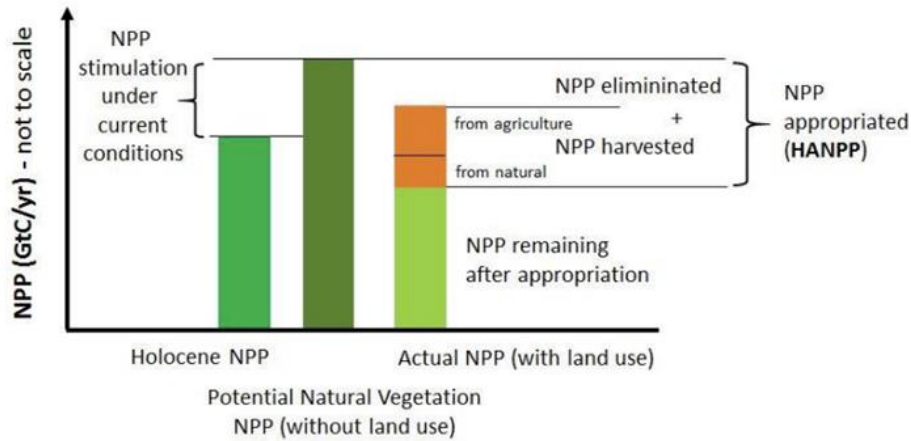


Figure 16. Schematic of the definition of HANPP used in Richardson et al. (2023), (not to scale) Source: (Richardson, et al., 2023), supplementary material.

Nevertheless, if a more detailed description of genetic variability in terms of number of species is required, the most feasible option would be to base it on the modelling structure used in the Felix model, which includes a biodiversity module.

4.4. Conclusions on planetary boundary modelling in WILLIAM

This section provides a summary table of all the planetary boundaries considered in the previous sections, including all the control variables proposed for each of them from different studies in the original and most current literature, as well as values of the thresholds that could be studied by the WILLIAM model. In addition, some conclusions related to the feasibility of studying the different planetary boundaries proposed in this framework are included at the end of the section.

Table 13. Summary of all planetary boundaries and proposed control variables. The control variables marked with an asterisk * are those proposed as an alternative or complement to the control variables proposed in Rockström et al. (2009) and Steffen et al. (2015).

Earth-system process	Control variable(s)	Units	Planetary boundary (Zone of uncertainty)	Current value of control variable
Climate change	Atmospheric CO ₂ concentration	[ppm]	Global scale: 350 ppm (350 - 550 ppm)	398.5 ppm CO ₂
	Energy imbalance at Earth's surface	[Wm ⁻²]	Global scale: +1.0 Wm ⁻² (+1.0 - +1.5 Wm ⁻²)	2.3 W m ⁻² (1.1–3.3 W m ⁻²)
	Change in global mean temperature since preindustrial times*	[°C]	Global scale: 1° (1-2°C) (Richardson, et al., 2023)	1.1°C
	Change in regional mean temperature	[°C]	Regional scale: -	-

		since preindustrial times*			
Ocean acidification		Carbonate ion concentration	[%]	Global scale: $\geq 80\%$ of the pre-industrial aragonite saturation state of mean surface ocean that is 3.44 Ω_{arag} (Richardson, et al., 2023), including natural diel and seasonal variability ($\geq 80 - \geq 70\%$)	2,8 Ω_{arag} (Richardson, et al., 2023)
		pH*	[dmnl]	Global scale: pH 7.80 (affecting mortality of adult decapod species (Bednaršek, et al., 2021)) This article provides more thresholds that affect different vital processes of these organisms.	Below pH 8.06 (Bednaršek, et al., 2021)
Biogeoc. flows	P	P flow from freshwater systems to oceans	[Tg P/yr]	Global scale: 11 Tg/yr (7-24 Tg/yr) (Carpenter & Bennett, 2011)	22,6 Tg/yr (Carpenter & Bennett, 2011)
		P flow from fertilizers to erodible soils	[Tg P/yr]	Regional scale: 6,2 Tg/yr (5,1-11,2 Tg/yr) (Liu, et al., 2013)	17,5 Tg/yr (Liu, et al., 2013)
	N	Industrial and intentional fixation of N	[Tg N/yr]	Global scale: 62 Tg/yr (30-70 Tg/yr) (de Vries et al., 2013)	190 Tg/yr (FAO, 2022)
Stratospheric ozone depletion		O ₃ concentration	[DU]	Global scale: <5% reduction from preindustrial level of 290 DU (5 – 10 %)	284.6 DU (Richardson, et al., 2023)
		EESC* (Equivalent effective stratospheric chlorine) concentration	[ppbv EESC]	Global scale: 3 ppb (WMO, 2022)	-
Atmospheric Aerosol Loading		AOD	[dmnl]	Regional scale: (South Asian Monsoon as a case study): anthropogenic total (absorbing and scattering) AOD over Indian subcontinent of 0.25 (0.25–0.50); absorbing (warming) AOD less than 10% of total AOD	0.30 AOD, over South Asian region
Land system change		Area of forested land as % or original forest cover	[%]	Global scale: 75% (75-54%) (values are a weighted average of the three individual biome boundaries and their uncertainty zones)	62%

			(Steffen, et al., 2015)	
	Area of forested land as % of potential forest	[%]	Global scale (aggregated): 75% (Richardson, et al., 2023) Tropical: 85% (85-60%) Temperate: 50% (50-30%) Boreal: 85% (85-60%) (Steffen, et al., 2015)	Global: 60%; tropical: Americas, 83.9%; Africa, 54.3%; Asia, 37.5%; temperate: Americas, 51.2%; Europe, 34.2%; Asia, 37.9%; boreal: Americas, 56.6%; Eurasia: 70.3% (Richardson, et al., 2023)
	Percentage of global land cover converted to cropland	[%]	Global scale: ≤15% of global ice-free land surface converted to cropland (15-20%) (Rockström, et al., 2009)	-
	Annual forest stock change (forest stock increment) *	[m ³ /yr]	Regional scale: see Figure 12. Average forestry boundaries of nations during 1991–2015. Source:Figure 12 (Zhang, et al., 2021)	In 2015, was 7.1 billion m ³ of forest stock increments
Fresh water use	Consumptive blue water use	[km ³ /yr]	Global scale: 4000 km ³ /yr (4000 – 6000 km ³ /yr)	2,600 km ³ /yr
Biosphere integrity	NPP*	[Gt of C/yr]	Global scale: 55.9 Gt of C/yr ± 1,1 Gt of C/yr (variation in Holocene). Risk evaluation: 10 – 20% of Holocene NPP (HANPP) (Richardson, et al., 2023)	71,4 Gt of C/yr (potential natural NPP) that is a 30% of HANPP (Richardson, et al., 2023)
Novel entities	?	?	?	Transgressed (Richardson, et al., 2023)

To conclude this section, it is possible to study some planetary boundaries with data from the WILLIAM model by adapting it slightly for the following cases: climate change, biosphere integrity, land system change, stratospheric ozone depletion and ocean acidification. The planetary boundaries of freshwater use, atmospheric aerosol loading and biogeochemical flows entail a greater modelling load since their study requires major changes in WILLIAM or even the generation of new submodules which, in addition, would contribute to the improvement of WILLIAM itself.

The planetary boundary of novel entities is currently difficult to study because of the lack of scientific consensus and limitations in terms lack of data as already mentioned in the previous sections, which does not allow for sufficient resources for introduction within WILLIAM.

5. Conclusions

This report describes the work done in Task 3.3. The main focus of task was the improvement of WILLIAM via three routes.

The first one, investigated a method to attribute the cause of changes to variables quantitatively. To assess the method's utility volcanoes and fires were used as toy models. This is described in Section 2.

The method was found sound for its purpose and could be used in some tasks of the WP4 (related to the assessment of impacts and risks).

Second, we analysed the ISIMIP data archive to incorporate its results into WILIAM. In particular, the effect of global warming on different variables such as average near-surface temperature, crop yields, methane emissions, etc. in all WILIAM regions are derived. Both median values as well as extremes are provided. All in all, 19 variables are analysed aiming at implementing them in the WILIAM model using damage functions, i.e. connecting such variables to climatic ones (CO₂ concentration or temperature change) and applying statistical analyses. We still work on one variable in the set, *forestry-npp*, and intend to explore whether other variables from the ISIMIP data base can be processed in a similar vein.

Aligned with this task was an exploration of a downscaling of ISIMIP impact data to the fine scales of the NEVERMORE case study areas. In particular, machine learning is used here. The approach has been used in Task 3.2 “Downscaling of climate information” for climate datasets and it will be tested in some ISIMIP variables.

Third, we investigated how the implementation of planetary boundaries improved. In particular the control variables and threshold values of them were looked at, and the feasibility of incorporating them into WILIAM was studied. In the end we found suitable control variables and their threshold values for all of them save one. The one that cannot be implemented is “novel entities.”

Overall, the team succeeded in carrying out the prescribed task and solutions to several tricky problems were found. We expect the collaboration of the partners to continue in the future and to yield further improvements for WILIAM.

6. References

- Agresti, A., & Finlay, B. (2009). *Statistical Methods for the Social Sciences*. Pearson International.
- Bednaršek, N., Ambrose, R., Calosi, P., Childers, R. K., Feely, R. A., Litvin, S. Y., . . . Weisberg, S. B. (2021). Synthesis of Thresholds of Ocean Acidification Impacts on Decapods. 8. doi:<https://doi.org/10.3389/fmars.2021.651102>
- Breach, P. A., & Simonovic, S. P. (2021). *ANEM13: A updated tool for global change analysis*.
- Burnham, K. P., & Anderson, D. R. (2002). *Model Selection and Multimodel Inference: A Practical Information-Theoretic Approach*. New York: Springer NY.
- Carpenter, S. R., & Bennett, E. M. (2011). Reconsideration of the planetary boundary for phosphorus. *Environmental Research Letters*, 6. doi:<https://doi.org/10.1088/1748-9326/6/1/014009>
- Chin, M., Diehl, T., Tan, Q., Prospero, J. M., Kahn, R. A., Remer, L. A., . . . Pan, X. (2014). Multi-decadal aerosol variations from 1980 to 2009: A perspective from observations and a global model. *Atmospheric Chemistry and Physics*, 14, 3657-3690. doi:<https://doi.org/10.5194/acp-14-3657-2014>
- Damkjaer, S., & Taylor, R. (2017, September). The measurement of water scarcity: Defining a meaningful indicator. *Ambio*, 46(5), 513–531. doi:10.1007/s13280-017-0912-z
- De Vries, W., Kros, J. K., & Seitzinger, S. P. (2013). Assessing planetary and regional nitrogen boundaries related to food security and adverse environmental impacts. *Current Opinion in Environmental Sustainability*, 5, 392-402. doi:<https://doi.org/10.1016/j.cosust.2013.07.004>

- Engle, R. F., & Granger, C. W. (1987). Cointegration and error correction: Representation, estimation, and testing. *Econometrica: Journal of the Econometric Society*, 251-276.
- Eyring, V., Bony, S., Meehl, G. A., Senior, C. A., S. B., Stouffer, R. J., & Taylor, K. E. (2016). Overview of the Coupled Model Intercomparison Project Phase 6. *Geosci. Model Dev.*, 9, 1937-1958,.
- FAO. (2022). *FAOSTAT: FAO database for food and agriculture*. Retrieved 4 19, 2022, from www.fao.org/faostat/
- Ferreras, N., Mateo, A., Vallejo, E., Lopez, P., Bartolomé, L., Karozis, S., . . . Fedele, G. (2023). *NEVERMORE Deliverable 3.1 Report on the improvements of the climate module of WILLIAM*.
- Frieler, K., Lange, S., Piontek, F., Reyer, C., & Schewe, J. (2017). Assessing the impacts of 1.5 °C global warming - simulation protocol of the Inter-Sectoral Impact Model Intercomparison Project (ISIMIP2b). *Geosific Model Development*, 4321-4345.
- Gleeson, T., Wang-Erlandsson, L., Z. S., Porkka, M., Jaramillo, F., Gerten, D., . . . Lehner, B. (2020). The Water Planetary Boundary: Interrogation and Revision. *One Earth*, 2, 223-234. doi:<https://doi.org/10.1016/j.oneear.2020.02.009>
- Granger, C. W. (1969). Investigating causal relations by econometric models and cross-spectral methods. *Econometrica: Journal of the Econometric Society*, 424-438.
- Granger, C. W., & Newbold, P. (1974). Spurious regressions in econometrics. *Journal of Econometrics*, 111-120.
- Hamilton, J. D. (1994). Granger causality. In J. D. Hamilton, *Time Series Analysis*. Princeton University Press.
- James, G., Witten, D., Hastie, T., & Tibshirani, R. (2013). *An Introduction to Statistical Learning*. Springer.
- Karozis, S., Klampanos, I. A., Sfetsos, A., & Vlachogiannis, D. (2023). A deep learning approach for spatial error correction of numerical seasonal weather prediction simulation data. *Big Earth Data*, 7, 231-250. doi:10.1080/20964471.2023.2172820
- Keeling, R. (2023). *Scripps Institution of Oceanography*. Retrieved from scrippsco2.ucsd.edu/
- Koellner, T., & Scholz, R. W. (2008). Assessment of land use impacts on the natural environment: Part 2: Generic characterization factors for local species diversity in Central Europe. *The International Journal of Life Cycle Assessment*, 13, 32-48. doi:<https://doi.org/10.1065/lca2006.12.292.2>
- Lade, S. J., Steffen, W., De Vries, W., Carpenter, S. R., Donges, J. F., Gerten, D., . . . Rockström, J. (2019). Human impacts on planetary boundaries amplified by Earth system interactions. *Nature Sustainability*, 3. doi:<https://doi.org/10.1038/s41893-019-0454-4>
- Lange, S., Volkholz, J., Geiger, T., Zhao, F., Vega, I., & Veldkamp, T. (2020). Projecting exposure to extreme climate impact events across six event categories and three spatial scales. *Earth's Future*.

- Liu, J., Zang, C., Tian, S., Liu, J., Yang, H., Jia, S., . . . Zhang, M. (2013). Water conservancy projects in China: Achievements, challenges and way forward. *Global Environmental Change*, 23, 633-643. doi:<https://doi.org/10.1016/j.gloenvcha.2013.02.002>
- Mechler, R., Bouwer, L. M., Schinko, T., Surminski, S., & Linnerooth-Bayer, J. (2019). *Loss and Damage from Climate Change: Concepts, Methods and Policy Options*. Springer International Publishing. doi:<https://doi.org/10.1093/reep/rez021>
- Meinshausen, M., Raper, S. C., & Wigley, T. M. (2011). Emulating coupled atmosphere-ocean and carbon cycle models with a simpler model, MAGICC6 – Part 1: Model description and calibration. *Atmospheric Chemistry and Physics*, 11, 1417-1456. doi:<https://doi.org/10.5194/acp-11-1417-2011>
- Moore, D. S., McCabe, G. P., & Craig, B. A. (2014). *Introduction to the Practice of Statistics*. W. H. Freeman.
- Neumann, J. E., Willwerth, J., Martinich, J., McFarland, J., Sarofim, M. C., & Yohe, G. (2020). Climate Damage Functions for Estimating the Economic Impacts of Climate Change in the United States. *Review of Environmental Economics and Policy*, 14, 25-43. doi:<https://doi.org/10.1093/reep/rez021>
- Newman, P. A., Daniel, J. S., Waugh, D. W., Nash, E. R., Miller, L. N., & Roberts, P. R. (2007). A new formulation of equivalent effective stratospheric chlorine (EESC). *Atmospheric Chemistry Physics*, 4537-4552.
- Pastor, A. V., Lourenço, T. C., Samsó, R., Martin, E., Ferreras, N., Ramos, I., & Papagianni, S. (2021). *LOCOMOTION Deliverable 6.3 Climate Change impacts and adaptation module*.
- Persson, L., Carney Almroth, B. M., Collins, C. D., Cornell, S., De Wit, C. A., Diamond, M. L., & Fantke, P. (2022, Hassellöv, M., MacLeod, M., Ryberg, M. W., Søgaard Jørgensen, P., Villarrubia-Gómez, P., Wang, Z., & Hauschild, M. Z. ()). Outside the Safe Oper). Outside the Safe Operating Space of the Planetary Boundary for Novel Entities. *Environmental Science & Technology*, 56, 1510-1521. doi:<https://doi.org/10.1021/acs.est.1c04158>
- Piontek, F., Kalkuhl, M., Kriegler, E., Schultes, A., Leimbach, M., Edenhofer, O., & Bauer, N. (2019). Economic Growth Effects of Alternative Climate Change Impact Channels in Economic Modeling. *Environmental and Resource Economics*, 73, 1357-1385. doi:<https://doi.org/10.1007/s10640-018-00306-7>
- Richardson, K., Steffen, W., Lucht, W., Bendtsen, J., Cornell, S. E., Donges, J. F., . . . Nogués-Bravo, D. (2023). Earth beyond six of nine planetary boundaries. *Science Advances*, 9. doi:<https://doi.org/10.1126/sciadv.adh2458>
- Rockström, J. P., Chapin, F. S., Lambin, E. F., Lenton, T. M., Scheffer, M., Folke, C., . . . Falkenmark, M. (2009). A safe operating for humanity. *Nature*, 461, 472-475. doi:<https://doi.org/10.1038/461472a>
- Rockström, J., Persson, Å., Chapin, F. S., Lambin, E. F., Lenton, T. M., Scheffer, M., . . . Falkenmark, M. (2009). A safe operating for humanity. *Nature*, 461, 472-475. doi:<https://doi.org/10.1038/461472a>

- Skeie, R., Fuglestvedt, J., Berntsen, T., Peters, G., & Andrew, G. (2017). Perspective has a strong effect on the calculation of historical contributions to global warming. Supplementary Material. *Environmental Research Letters*.
- Snyder, A., Calvin, K., Clarke, L., Edmonds, J., & Kyle, P. (2020). The domestic and international implications of future climate for U.S. agriculture in GCAM. *PLoS ONE*, 15. doi:<https://doi.org/10.1371/journal.pone.0237918>
- Steffen, W., Richardson, K., Rockström, J., Cornell, S. E., Fetzer, I., Bennett, E. M., . . . Sörlin, S. (2015). Planetary boundaries: Guiding human development on a changing planet. *Science*, 347. doi:<https://doi.org/10.1126/science.1259855>
- Streets, D. G., Yan, F., Chin, M., Diehl, T., Mahowald, N., Schultz, M., . . . Wu, Y. Y. (2009). Anthropogenic and natural contributions to regional trends in aerosol optical depth, 1980–2006. *Journal of Geophysical Research*, 114. doi:<https://doi.org/10.1029/2008JD011624>
- Tans, P. (2023). *NOAA/GML*. Retrieved from gml.noaa.gov/ccgg/trends/
- Taylor, K., Stouffer, R., & Meehl, G. (2012). An Overview of CMIP5 and the experiment design. *Bull. Amer. Meteor. Soc*, 93, 485-498.
- Wang-Erlandsson, L., Tobian, A., Van Der Ent, R. J., Fetzer, I., Te Wierik, S., Porkka, M., . . . Rockström, J. (2022). A Planetary Boundary for Green Water. *Nature Reviews Earth & Environment*, 3, 380-392. doi:<https://doi.org/10.1038/s43017-022-00287-8>
- WMO. (2022). *Executive Summary: Scientific Assessment of Ozone Depletion*. Geneva: WMO.
- Zhang, H., Liu, C., Wang, C., Ying, Z., Lu, C., & Chen, G. (2021). Extreme climate events and economic impacts in China: A CGE analysis with a new damage function in IAM. *Technological Forecasting and Social Change*, 169. doi:<https://doi.org/10.1016/j.techfore.2021.120765>



Contacts

Fondazione Bruno Kessler

E-mail: nevermore-communication@fbk.eu

Phone: +39 0461 314444

Fax: +39 0461 314444

via Sommarive, 18,
cp: 38123 Povo TN, Italia



This project has received funding from the European Union's Horizon Europe research and innovation programme under grant agreement No 101056858.